International Journal of Innovation and Applied Studies
ISSN 2028-9324 Vol. 1 No. 1 Nov. 2012, pp. 118-152

http://www.issr-journals.org/ijias/

Radiation Effects on Convective Heat and Mass Transfer Flow in a Rectangular Cavity

A. Veera Suneela Rani[1], Dr. V. Sugunamma[2], and N. Sandeep[1]

[1]Research Scholars, Department of Mathematics,
S. V. University,
Tirupati, A.P., India

[2]Associate Professor, Department of Mathematics,
S. V. University,
Tirupati, A.P., India

ABSTRACT: In this paper we analyze the combine influence of radiation and dissipation on the convective heat and mass transfer flow of a viscous fluid through a porous medium in a rectangular cavity using Darcy model. Making use of the incompressibility the governing non-linear coupled equations for the momentum, energy and diffusion are derived in terms of the non-dimensional stream function, temperature and concentration. The Galerkin finite element analysis with linear triangular elements is used to obtain the Global stiffness matrices for the values of stream function, temperature and concentration. These coupled matrices are solved using iterative procedure and expressions for the stream function, temperature and concentration are obtained as linear combinations of the shape functions. The behavior of temperature, concentration, Nusselt number and Sherwood number are discussed computationally for different values of the governing Parameters Ra, α, N, N_1, Sc, S_0 and Ec.

KEYWORDS: Radiation, Heat and Mass Transfer, Porous Medium, Galerkin Finite Element Analysis.

1 INTRODUCTION

The study of heat transfer and mixed convection flow in porous medium enclosures of various shapes has received much attention [1]-[5]. Interest in these natural convection flow and heat transfer in porous medium has been motivated by a broad range of applications, including Geothermal systems, Crude oil production, storage of Nuclear waste materials, ground water pollution, fiber and granular insulations. solidification of castings, etc. In a wide range of such problems, the physical system can be modeled as a two-dimensional rectangular enclosure withy vertical walls held at different temperatures and the connecting horizontal walls considered adiabatic. Convective heat transfer in a Rectangular porous duct whose vertical walls are maintained at two different temperatures and horizontal walls insulated, is a problem which has received attention by many investigators [6]-[13] some of these works includes numerical results by a few authors [5], [14]-[23].

The investigation of heat transfer in enclosures containing porous media began with the experimental work of Verschoor and Greebler [24]. Verschoor and Greebler [24] were followed by several other investigators interested in porous media heat transfer in rectangular enclosures [12]-[13], [25]-[26]. In particular Bankvall [1]-[2], [27] has published a great deal of practical work concerning heat transfer by natural convection in rectangular enclosures completely filled with porous media. Burns, Chow-and Tien [28] have described a porous medium heat transfer flow in a rectangular geometry. Cheng et. al. [16] have studied the flow and heat transfer rate in a rectangular box with solid walls using a Brinkman model the box is differentially heated in the horizontal direction. Chen et. al. [17] have considered enclosures with aspect ratio greater than or equal to one. Their numerical computations indicate that when Darcy number based on the width of the enclosures is less than 10^{-9}, Darcy's law and the Brinkman equation virtually the same results for the heat transfer rate. Joseph *et. al.,* [19] have considered laminar forced convection in rectangular channels with unequal heat addition on adjacent sides. Teomann Ay Han et. al., [29] have considered heat transfer and flow structure in a rectangular channel with wing-type Vortex Generator. Han-Chieh Chiu et. al., [30] have discussed mixed convection heat transfer in horizontal rectangular ducts with radiation effects. Chitti Babu et. al., [31] has discussed convective flow in a porous rectangular duct with differentially heated side wall using Brinkman model.

When heat and mass transfer occur simultaneously, it leads to complex fluid motion called double-diffusive convection. Double-diffusion occurs in a wide range of scientific fields such as oceanography, astrophysics, geology, biology and chemical processes. Ostrich [32] and Viskanta et. al., [33] reported complete reviews on the subject. Bejan [14] reported fundamental study of scale analysis relative to heat and mass transfer with in cavities submitted to horizontal combined and pure temperature and concentration gradients. Kamotain *et. al.,* [21] have conducted experiments on mass transfer and flow pattern in shallow enclosures [H\L = 0, 13-0.55] filled with a fluid [P_r = 7, Sc = 2100] in cases where the combined buoyancy effect is dominated by the buoyancy due to concentration gradient. Other experimental studies dealing with thermo solutal convection in rectangular enclosures were reported by Ostrach *et. al.,* [32] and Lee *et. al.,* [34]. Lee and Hyun [34] and Hyun and Lee [35] reported numerical solutions for unsteady double-diffusive convection in a rectangular enclosure with aiding and opposing temperature and concentration gradients that were in good agreement with reported experimental results. The most recent review of this activity is the one published by Viskanta *et. al.,* [33]. Who stress that the two requirements for the occurrence of double-diffusive convection are that the fluid contain two or more components with different molecular diffusivities and that these components make opposing contributions to the vertical density gradients. Trevisan and Bejan [36] have analyzed the natural convection caused by analytically and numerically in a rectangular enclosure with uniform heat and mass fluxes along the vertical sides. He obtained o seen linearised solution for all spaces filled with mixtures characterized by Le = 1 and arbitrary buoyancy ratios.

The effect of varying the Lewis number (L) is documented by a similarity solution valid for Le > 1 in heat transfer driven flows and for Le < 1 mass transfer driven flows. Mass line patterns are used to visualize the convective mass transfer rate and the flow reversal is observed when the buoyancy ratio n = 1. Also Trevisan *et. al.,* [37] have studied natural convection heat and mass transfer through a vertical porous layer subjected to uniform fluxes of heat and mass from the side. The Oseen's Linearized solution that yielded the overall heat and mass transfer correlation was developed for porous medium and a buoyancy effect ruled by both temperature and concentration variations in the high Rayleigh number region where the heat and mass transfer rates differ greatly from estimates based on the assumption of pure diffusion. The similarity solution that produced the overall mass transfer was developed for different parametric domain.

Literature suggests that the effect of viscous dissipation on heat transfer as been studied for different geometries. Brinkman [38], have studied the viscous dissipation effect on natural convection in horizontal cylinder embedded in porous medium. Their study showed that the viscous dissipation effect on natural convection in a porous cavity and found that the heat transfer rate at hot surface decreases with increase of viscous dissipation parameter. Thermal radiation plays a significant role in the overall surface heat transfer where convective heat transfer is small. Verschoor *et. al.,* [39] have studied the effect of viscous dissipation and radiation on unsteady magneto hydrodynamic free convection flow fast vertical plate in porous medium. They found that the temperature profile increases when viscous dissipation increases. A good amount of work has been done to understand natural convection in porous cavity. Inspite of endeavour efforts to study heat transfer in porous cavity, the combined effect of viscous dissipation and radiation on porous medium filled inside a square cavity has not received attention. Badruddin *et. al.,* [40] have investigated the radiation and viscous dissipation on convective heat transfer in porous cavity. Recently Padmavathi [8] Nagaradhika [41] and Sreenivas have analyzed the connective heat transfer through a porous medium in a rectangular cavity with heat sources and dissipation under varied conditions. Ranga Reddy [11] has discussed the natural convective Heat and Mass transfer in Porous Rectangular Cavity with a differentially heated side walls using Brinkman model. By using Galerkin finite element analysis, the governing equations are solved. Sivaiah *et. al.,* [13] have investigated double-diffusive convective Heat transfer flow of a viscous fluid through a porous medium with rectangular duct with thermo-diffusion by using finite element technique. Reddaiah *et. al.,* [42] have analyzed the effect of viscous dissipation on convective heat and mass transfer flow of a viscous fluid in a duct of rectangular cross section by employing Galerkin finite element analysis. Recently Shanthi [37] has discussed the mixed convective heat and mass transfer flow of a viscous fluid through a porous medium in a rectangular duct with Soret effect.

In this paper an attempt has been made to discuss the combine influence of radiation and dissipation on the convective heat and mass transfer flow of a viscous fluid through a porous medium in a rectangular cavity using Darcy model. Making use of the incompressibility the governing non-linear coupled equations for the momentum, energy and diffusion are derived in terms of the non-dimensional stream function, temperature and concentration. The Galerkin finite element analysis with linear triangular elements is used to obtain the Global stiffness matrices for the values of stream function, temperature and concentration. These coupled matrices are solved using iterative procedure and expressions for the stream function, temperature and concentration are obtained as a linear combinations of the shape functions. The behaviour of temperature, concentration, Nusselt number and Sherwood number are discussed computationally for different values of the governing Parameters Ra, α, N, N_1, Sc, S_0 and Ec.

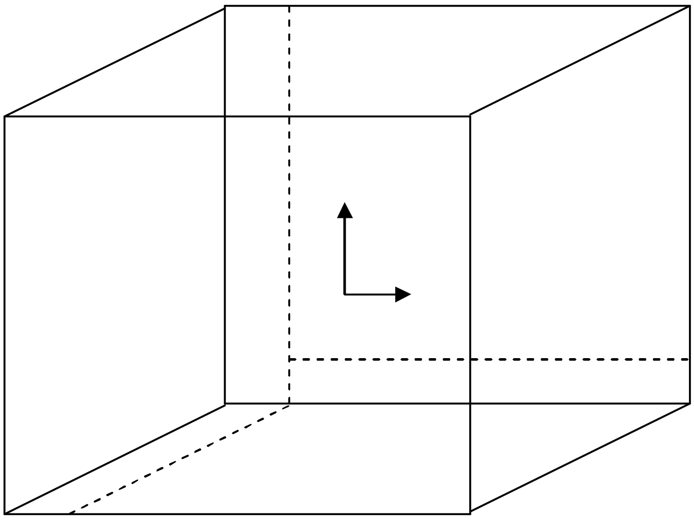

Fig. 1. Schematic diagram of the flow model

2 FORMULATION OF THE PROBLEM

We consider the mixed convective heat and mass transfer flow of a viscous incompressible fluid in a saturated porous medium confined in the rectangular duct (Fig. 1) whose base length is a and height b. The heat flux on the base and top walls is maintained constant. The Cartesian coordinate system O (x,y) is chosen with origin on the central axis of the duct and its base parallel to x-axis.

We assume that

i) The convective fluid and the porous medium are everywhere in local thermodynamic equilibrium.
ii) There is no phase change of the fluid in the medium.
iii) The properties of the fluid and of the porous medium are homogeneous and isotrophic.
iv) The porous medium is assumed to be closely packed so that Darcy's momentum law is adequate in the porous medium.
v) The Boussinesq approximation is applicable.

Under these assumption the governing equations are given by:

$$\frac{\partial u'}{\partial x'}+\frac{\partial v'}{\partial y'}=0 \tag{2.1}$$

$$u'=-\frac{k}{\mu}\left(\frac{\partial p'}{\partial x'}\right) \tag{2.2}$$

$$v'=-\frac{k}{\mu}\left(\frac{\partial p'}{\partial y'}+\rho' g\right)-(\frac{\sigma\mu_e^2H_o^2k}{\mu})v' \tag{2.3}$$

$$\rho_\sigma c_p\left(u'\frac{\partial T'}{\partial x'}+v'\frac{\partial T'}{\partial y'}\right)=K_1\left(\frac{\partial^2T'}{\partial x'^2}+\frac{\partial^2T'}{\partial y'^2}\right)+Q(T_0-T)+\left(\frac{\mu}{K}\right)(u^2+v^2)-\frac{\partial(q_r)}{\partial x} \tag{2.4}$$

$$\rho_\sigma c_p\left(u'\frac{\partial C}{\partial x'}+v'\frac{\partial C}{\partial y'}\right)=D_1\left(\frac{\partial^2C}{\partial x'^2}+\frac{\partial^2C}{\partial y'^2}\right)+k_{11}\left(\frac{\partial^2T}{\partial x'^2}+\frac{\partial^2T}{\partial y'^2}\right) \tag{2.5}$$

$$\rho' = \rho_0 \left\{1 - \beta(T' - T_0)\, \beta^{\bullet}(C' - C_0)\right\} \tag{2.6}$$
$$T_0 = \frac{T_h + T_c}{2}, C_0 = \frac{C_h + C_c}{2}$$

where u′ and v′ are Darcy velocities along θ(x, y) direction. T′, C,p′ and g′ are the temperature, Concentration, pressure and acceleration due to gravity, T_c ,Cc and T_h ,C_h are the temperature and Concentration on the cold and warm side walls respectively. ρ′, μ, ν, and β are the density, coefficients of viscosity, kinematic viscosity and thermal expansion of he fluid, k is the permeability of the porous medium, K_1 is the thermal conductivity, C_p is the specific heat at constant pressure , Q is the strength of the heat source,k_{11} is the cross diffusivity , β* is the volume coefficient of expansion with mass fraction concentration , σ is the electrical conductivity , μ_e is the magnetic permeability of the medium ,Ho is the strength of the magnetic field and q_r is the radiative heat flux..

The boundary conditions are:

u′ = v′ = 0	on the boundary of the duct	
$T' = T_c$, $C=C_c$	on the side wall to the left	
$T' = T_h$, $C=C_h$	on the side wall to the right	(2.7)
$\frac{\partial T'}{\partial y} = 0$, $\frac{\partial C}{\partial y} = 0$	on the top (y = 0) and bottom	
$u = v = 0$	walls(y = 0)which are insulated.	

Invoking Rosseland approximation for radiation:

$$q_r = \frac{4\sigma^*}{3\beta_R}\frac{\partial T'^4}{\partial y}$$

Expanding T^4 in Taylor's series about T_e and neglecting higher order terms:

$$T'^4 \cong 4T_e^3 T - 3T_e^4$$

We now introduce the following non-dimensional variables:

x′ = ax; ;	y′ = by ;	c = b/a
u′ = (ν/a) u ;	v′ = (ν/a)v ;	$p' = (\nu^2\rho/a^2)p$
$T' = T_0 + \theta\,(T_h - T_c)$		$C' = C_0 + \phi\,(T_h - T_c)$ (2.8)

The governing equations in the non-dimensional form are:

$$u = -\left(\frac{K}{a^2}\right)\frac{\partial p}{\partial x} \tag{2.9}$$

$$v = -\frac{k}{a^2}\frac{\partial p}{\partial y} - \frac{kag}{v^2} + \frac{kag\beta(T_h - T_c)\theta}{v^2} + \frac{kag\beta^{\bullet}(C_h - C_c)\phi}{v^2} - \left(\frac{\sigma\mu_e^2 H_o^2 k}{\mu}\right)v \tag{2.10}$$

$$P\left(u\frac{\partial\theta}{\partial x} + v\frac{\partial\theta}{\partial y}\right) = \left(1 + \frac{4N}{3}\right)\left(\frac{\partial^2\theta}{\partial x^2} + \frac{\partial^2\theta}{\partial y^2}\right) - \alpha\theta + E_C\left(u^2 + v^2\right) \tag{2.11}$$

$$Sc\left(u\frac{\partial\phi}{\partial x} + v\frac{\partial\phi}{\partial y}\right) = \left(\frac{\partial^2\phi}{\partial x^2} + \frac{\partial^2\phi}{\partial y^2}\right) + \frac{ScSo}{N}\left(\frac{\partial^2\theta}{\partial x^2} + \frac{\partial^2\theta}{\partial y^2}\right) \tag{2.12}$$

In view of the equation of continuity we introduce the stream function ψ as:

$$u = \frac{\partial\psi}{\partial y} \;;\quad v = -\frac{\partial\psi}{\partial x} \tag{2.13}$$

Eliminating p from the equation (2.9) and (2.10) and making use of (2.11) the equations in terms of ψ and θ are:

$$\nabla^2\psi - M_1^2\frac{\partial^2\psi}{\partial x^2} = -Ra(\frac{\partial\theta}{\partial x} + N\frac{\partial\phi}{\partial x}) \tag{2.14}$$

$$P\left(\frac{\partial\psi}{\partial y}\frac{\partial\theta}{\partial x} - \frac{\partial\psi}{\partial x}\frac{\partial\theta}{\partial y}\right) = \left(1+\frac{4}{3N_1}\right)\left(\frac{\partial^2\theta}{\partial x^2}+\frac{\partial^2\theta}{\partial y^2}\right) - \alpha\theta + E_C\left(\left(\frac{\partial\psi}{\partial y}\right)^2 + \left(\frac{\partial\psi}{\partial x}\right)^2\right) \tag{2.15}$$

$$Sc\left(\frac{\partial\psi}{\partial y}\frac{\partial\phi}{\partial x} - \frac{\partial\psi}{\partial x}\frac{\partial\phi}{\partial y}\right) = \left(\frac{\partial^2\phi}{\partial x^2}+\frac{\partial^2\phi}{\partial y^2}\right) + \frac{ScSo}{N}\left(\frac{\partial^2\theta}{\partial x^2}+\frac{\partial^2\theta}{\partial y^2}\right) \tag{2.16}$$

Where:

$G = \frac{g\beta(T_h - T_c)a^3}{\nu^2}$ (Grashof number), $D^{-1} = \frac{a^2}{k}$ (Darcy parameter)

$M^2 = \frac{\sigma\mu_e^2 H_o^2 a^2}{\nu^2}$ (Hartmann Number), $P = \mu\, c_p / K_1$(Prandtl number)

$\alpha = Qa^z/K_1$ (Heat source parameter), $Ra = \frac{\beta g(T_g - T_c)ka}{\nu^2}$ (Radiation parameter)

$N_1 = \frac{3\beta_R K_1}{4\sigma^\bullet : T_e^3}$ (Rayleigh Number), $Sc = \frac{\nu}{D}$ (Schmidt Number)

$So = \frac{k_{11}\beta^\bullet}{\nu\beta}$ (soret parameter), $N = \frac{\beta^*(C_h - C_c)}{\beta(T_h - T_c)}$ (Buoyancy ratio)

$Ec = \left(\frac{a^4}{\mu K K_1 \Delta T}\right)$ (Eckert number)

The four boundary conditions are:

$$\frac{\partial\psi}{\partial x} = 0, \frac{\partial\psi}{\partial y} = 0 \ on \quad x = 0 \ \& 1 \tag{2.17}$$

$$\theta = 1 \quad \phi = 1 \quad on \quad x = 0$$

$$\theta = 0 \quad \phi = 0 \quad on \quad x = 1 \tag{2.18}$$

3 FINITE ELEMENT ANALYSIS AND SOLUTION OF THE PROBLEM

The region is divided into a finite number of three node triangular elements, in each of which the element equation is derived using Galerkin weighted residual method. In each element f_i the approximate solution for an unknown f in the variational formulation is expressed as a linear combination of shape function. $(N_k^i)k = 1,2,3,$ Which are linear polynomials in x and y. This approximate solution of the unknown f coincides with actual values at each node of the element. The variational formulation results in a 3 x 3 matrix equation (stiffness matrix) for the unknown local nodal values of the given element. These stiffness matrices are assembled in terms of global nodal values using inter element continuity and boundary conditions resulting in global matrix equation.

In each case there are r distinct global nodes in the finite element domain and f_p (p = 1,2,……r) is the global nodal values of any unknown f defined over the domain then:

$$f=\sum_{i=1}^{8}\ \sum_{p=1}^{r} f_p\ \Phi_{\mathrm{p}}^{\mathrm{i}}\ ,$$

Where the first summation denotes summation over s elements and the second one represents summation over the independent global nodes and:

$\Phi_p^i = N_N^i$, if p is one of the local nodes say k of the element e_i

= 0, otherwise.

f_p' s are determined from the global matrix equation. Based on these lines we now make a finite element analysis of the given problem governed by (2.14)- (2.16) subjected to the conditions (2.17) – (2.18).

Let ψ^i, θ^i and ϕ^i be the approximate values of ψ ,θ and ϕ in an element θ_i.

$$\psi^i = N_1^i\ \psi_1^i + N_2^i\ \psi_2^i + N_3^i\ \psi_3^i \tag{3.1a}$$

$$\theta^i = N_1^i\ \theta_1^i + N_2^i\ \theta_2^i + N_3^i\ \theta_3^i \tag{3.1b}$$

$$\phi = N_1^i\ \phi_1^i + N_2^i\ \phi_2^i + N_3^i\ \phi_3^i = \tag{3.1c}$$

Substituting the approximate value ψ^i, θ^i and ϕ^i for ψ ,θ and ϕ respectively in (2.13), the error:

$$E_1^i = \left(1+\frac{4}{3N_1}\right)\frac{\partial^2\theta^i}{\partial x^2}+\frac{\partial^2\theta^i}{\partial y^2}-P\left(\frac{\partial\psi^i}{\partial y}\ \frac{\partial\theta^i}{\partial x}\ -\frac{\partial\psi^i}{\partial x}\ \frac{\partial\theta^i}{\partial y}\right)-\alpha\theta+E_C\left[\left(\frac{\partial\psi}{\partial y}\right)^2+\left(\frac{\partial\psi}{\partial x}\right)^2\right] \tag{3.2}$$

$$E_2^i = \frac{\partial^2\phi^i}{\partial x^2}+\frac{\partial^2\phi^i}{\partial y^2}-Sc\left(\frac{\partial\psi^i}{\partial y}\ \frac{\partial\phi^i}{\partial x}\ -\frac{\partial\psi^i}{\partial x}\ \frac{\partial\phi^i}{\partial y}\right)+\frac{ScSo}{N}\left(\frac{\partial^2\phi^i}{\partial x^2}+\frac{\partial^2\phi^i}{\partial y^2}\right) \tag{3.3}$$

Under Galerkin method this error is made orthogonal over the domain of e_i to the respective shape functions (weight functions) where:

$$\int_{ei} E_1^i\ N_k^i\ d\Omega\ =0$$

$$\int_{ei} E_2^i N_k^i d\Omega=0$$

$$\begin{aligned}\int_{ei=} N_k^i(&\left(1+\frac{4}{3N_1}\right)\left(\frac{\partial^z\theta^i}{\partial x^2}+\frac{\partial^z\theta^i}{\partial y^2}\right)-P\left(\frac{\partial\psi^i}{\partial y}\ \frac{\partial\theta^i}{\partial x}\ -\frac{\partial\psi^i}{\partial x}\ \frac{\partial\theta^i}{\partial y}\right)\\ &-\alpha\theta+\left[E_C\left(\frac{\partial\psi}{\partial y}\right)^2+\left(\frac{\partial\psi}{\partial x}\right)^2\right]d\Omega=0\end{aligned} \tag{3.4}$$

$$\begin{aligned}\int_{ei=} N_k^i(&\left(\frac{\partial^z\phi^i}{\partial x^2}+\frac{\partial^z\phi^i}{\partial y^2}\right)-Sc\left(\frac{\partial\psi^i}{\partial y}\ \frac{\partial\phi^i}{\partial x}\ -\frac{\partial\psi^i}{\partial x}\ \frac{\partial\phi^i}{\partial y}\right)\\ &+\frac{ScSo}{N}\left(\frac{\partial^z\theta^i}{\partial x^2}+\frac{\partial^z\theta^i}{\partial y^2}\right)d\Omega=0\end{aligned} \tag{3.5}$$

Using Green's theorem we reduce the surface integral (3.4) & (3.5) without affecting ψ terms and obtain:

$$\int_{ei} N_k^i \left\{ \begin{array}{l} \left(1+\frac{4}{3N_1}\right)\frac{\partial N_k^i}{\partial x}\frac{\partial \theta^i}{\partial x}+\frac{\partial N_k^i}{\partial y}\frac{\partial \theta^i}{\partial y} - p^i N_k\left(\frac{\partial \psi^i}{\partial y}\frac{\partial \theta^i}{\partial x}-\frac{\partial \psi^i}{\partial x}\frac{\partial \theta^i}{\partial y}\right) \\ \qquad -\alpha\theta + E_C\left(\frac{\partial \psi}{\partial y}\right)^2+\left(\frac{\partial \psi}{\partial x}\right)^2 \end{array} \right\} d\Omega$$

$$= \int_{\Gamma i} N_k^i \left(\frac{\partial \theta^i}{\partial x} n_x + \frac{\partial \theta^i}{\partial y} n_y \right) d\Gamma_i \tag{3.6}$$

$$\int_{eiei} N_k^i \left\{ \frac{\partial N_k^i}{\partial x}\frac{\partial \phi^i}{\partial x}+\frac{\partial N_k^i}{\partial y}\frac{\partial \phi^i}{\partial y} - Sc^i N_k\left(\frac{\partial \psi^i}{\partial y}\frac{\partial \phi^i}{\partial x}-\frac{\partial \psi^i}{\partial x}\frac{\partial \phi^i}{\partial y}\right) + \frac{ScSo}{N}(^2\frac{\partial N_k^i}{\partial x}\frac{\partial \theta^i}{\partial x}+\frac{\partial N_k^i}{\partial y}\frac{\partial \theta^i}{\partial y}) \right\} d\Omega$$

$$= \int_{\Gamma i} N_k^i \left(\frac{\partial \theta^i}{\partial x} + \frac{ScSo}{N}\frac{\partial \phi^i}{\partial x})n_x + (\frac{\partial \theta^i}{\partial y} + \frac{ScSo}{N}\frac{\partial \phi^i}{\partial y} n_y \right) d\Gamma_i \tag{3.7}$$

Where Γ_I is the boundary of e_i.

Substituting L.H.S. of (3.1a)- (3.1c) for ψ^i, θ^i and ϕ^i in (3.6)&(3.7) we get:

$$\sum_1 \int_{ei} \left(1+\frac{4N}{3}\right)\frac{\partial N_k^i}{\partial x}\frac{\partial N_L^i}{\partial x}+\frac{\partial N_L^i}{\partial y}\frac{\partial N_k^i}{\partial y} - P\sum_1 \psi_m^i \int_{ei}\left(\frac{\partial N_m^i}{\partial y}\frac{\partial N_L^i}{\partial x}-\frac{\partial N_m^i}{\partial x}\frac{\partial N_L^i}{\partial y}\right)d\Omega$$

$$-\alpha \sum \theta^i \int_{ei} N_k N_l \, d\Omega_i + E_C \int_{ei}\left(\left(\frac{\partial \psi}{\partial y}\right)^2+\left(\frac{\partial \psi}{\partial x}\right)^2\right)d\Omega$$

$$= \int_{\Gamma_i} N_k^i \left(\frac{\partial \theta^i}{\partial x} n_x + \frac{\partial \theta^i}{\partial y} n_y \right) d\Gamma_i = Q_k^i \qquad (l,\ m,\ k = 1,2,3) \tag{3.8}$$

$$\sum_1 \int_{ei} \phi^i (\frac{\partial N_k^i}{\partial x}\frac{\partial N_L^i}{\partial x}+\frac{\partial N_L^i}{\partial y}\frac{\partial N_k^i}{\partial y}) - Sc\sum_1 \psi_m^i \int_{ei}\left(\frac{\partial N_m^i}{\partial y}\frac{\partial N_L^i}{\partial x}-\frac{\partial N_m^i}{\partial x}\frac{\partial N_L^i}{\partial y}\right)d\Omega$$

$$+\frac{ScSo}{N}\sum \theta^i \int_{ei} (\frac{\partial N_k^i}{\partial x}\frac{\partial N_L^i}{\partial x}+\frac{\partial N_L^i}{\partial y}\frac{\partial N_k^i}{\partial y}) d\Omega_i^{\ i}$$

$$= \int_{\Gamma i} N_k^i \left(\frac{\partial \theta^i}{\partial x} + \frac{ScSo}{N}\frac{\partial \phi^i}{\partial x})n_x + (\frac{\partial \theta^i}{\partial y} + \frac{ScSo}{N}\frac{\partial \phi^i}{\partial y} n_y \right) d\Gamma_i = Q_i^C \qquad (l,\ m,\ k = 1,2,3) \tag{3.9}$$

Where:

$Q_k^i = Q_{k1}^i + Q_{k2}^i + Q_{k3}^i, Q_k^i$'s being the values of Q_k^i on the sides s = (1,2,3) of the element e_i. The sign of Q_k^i's depends on the direction of the outward normal w.r.t the element.

Choosing different N_k^i's as weight functions and following the same procedure we obtain matrix equations for three unknowns (Q_p^i) viz.,

$$(a_p^i)(\theta_p^i) = (Q_k^i) \tag{3.10}$$

Where (a_{pk}^i) is a 3 x 3 matrix, $(\theta_p^i), (Q_k^i)$ are column matrices.

Repeating the above process with each of s elements, we obtain sets of such matrix equations. Introducing the global coordinates and global values for θ_p^i and making use of inter element continuity and boundary conditions relevant to the problem the above stiffness matrices are assembled to obtain a global matrix equation. This global matrix is r x r square matrix if there are r distinct global nodes in the domain of flow considered.

Similarly substituting ψ^i, θ^i and ϕ^i in (2.12) and defining the error:

$$E_3^i = \nabla^2\psi - M^2\psi + \mathrm{Ra}\,(\frac{\partial\theta}{\partial \mathrm{x}} + N\frac{\partial\phi}{\partial \mathrm{x}}) \tag{3.11}$$

And following the Galerkin method we obtain:

$$\int_\Omega E_3^i \psi_j^i d\Omega = 0 \tag{3.12}$$

Using Green's theorem (3.8) reduces to:

$$\int_\Omega \left(\frac{\partial N_k^i}{\partial x}\frac{\partial \psi^i}{\partial x} + \frac{\partial N_k^i}{\partial y}\frac{\partial \psi^i}{\partial y} + \mathrm{Ra}\,(\theta^i \frac{\partial N_k^i}{\partial x} + \phi^i \frac{\partial N_k^i}{\partial x} \right) d\Omega$$

$$= \int_\Gamma N_k^i \left(\frac{\partial \psi^i}{\partial x} n_x + \frac{\partial \psi^i}{\partial y} n_y \right) d\Gamma_i + \int_\Gamma N_k^i n_x \theta^i d\Gamma_i \tag{3.13}$$

In obtaining (3.13) the Green's theorem is applied w.r.t derivatives of ψ without affecting θ terms.

Using (3.1) and (3.2) in (3.13) we have:

$$\sum_m \psi_m^i \left\{ \int_\Omega \left(\frac{\partial N_k^i}{\partial x}\frac{\partial N_m^i}{\partial x} + \frac{\partial N_m^i}{\partial y}\frac{\partial N_k^i}{\partial y} \right) d\Omega_i + \mathrm{Ra}\sum_L (\theta_L^i \int_{\Omega_i} \mathrm{N}_\mathrm{k}^\mathrm{i} \frac{\partial N_L^i}{\partial x} d\Omega + \phi_L^i N \int_{\Omega_i} \mathrm{N}_\mathrm{k}^\mathrm{i} \frac{\partial N_L^i}{\partial x} d\Omega \right\}$$

$$= \int_\Gamma N_k^i \left(\frac{\partial \psi^i}{\partial x} n_x + \frac{\partial \psi^i}{\partial y} n_y \right) d\Gamma_i + \int_\Gamma N_k^i \theta^i d\Omega_i = \Gamma_k^i \tag{3.14}$$

In the problem under consideration, for computational purpose, we choose uniform mesh of 10 triangular elements (Fig. 2). The domain has vertices whose global coordinates are (0,0), (1,0) and (1,c) in the non-dimensional form. Let e_1, e_2.....e_{10} be the ten elements and let θ_1, θ_2, ...θ_{10} be the global values of θ and ψ_1, ψ_2,......ψ_{10} be the global values of ψ at the ten global nodes of the domain (Fig. 2).

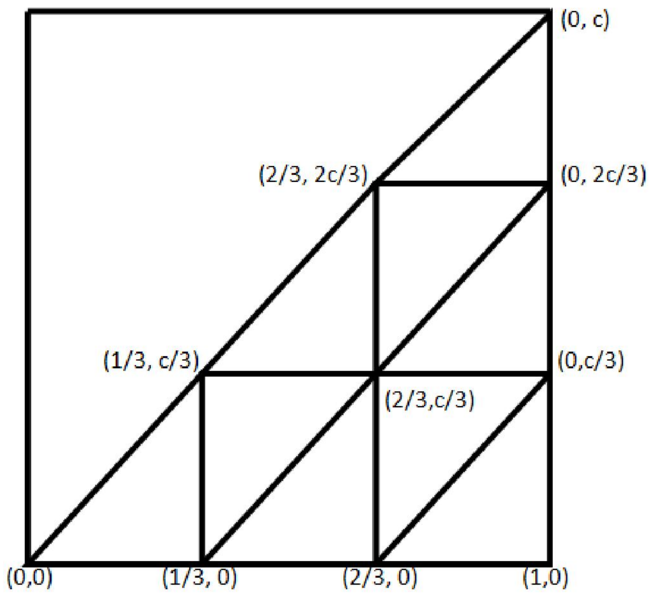

Fig. 2. Schematic diagram of the configuration

4 SHAPE FUNCTIONS AND STIFFNESS MATRICES

Range functions in $\underset{i,j}{n}$; *i* = element, *j* = node.

$\underset{1,1}{n} = 1 - 3x$

$\underset{1,2}{n} = 3x - \dfrac{3y}{C}$

$\underset{2,1}{n} = 1 - \dfrac{3y}{C}$

$\underset{2,2}{n} = -1 + \dfrac{3y}{C}$

$\underset{2,3}{n} = 1 - 3x + \dfrac{3y}{C}$

$\underset{3,1}{n} = 2 - 3x$

$\underset{3,2}{n} = -1 + 3x - \dfrac{3y}{C}$

$\underset{3,3}{n} = \dfrac{3y}{C}$

$\underset{4,1}{n} = 1 - \dfrac{3y}{C}$

$\underset{4,2}{n} = -2 + 3x$

$\underset{4,3}{n} = 2 - 3x + \dfrac{3y}{C}$

$\underset{5,1}{n} = 2 - 3x$

$\underset{5,2}{n} = -1 + 3x - \dfrac{3y}{C}$

$\underset{5,3}{n} = \dfrac{3y}{C}$

$\underset{6,1}{n} = 2 - 3x$

$\underset{6,2}{n} = 3x - \dfrac{3y}{C}$

$\underset{6,3}{n} = 1 + \dfrac{3y}{C}$

$\underset{7,1}{n} = 2 - \dfrac{3y}{C}$

$\underset{7,2}{n} = -2 + 3x$

$\underset{7,3}{n} = 1 - 3x + \dfrac{3y}{C}$

$\underset{8,1}{n} = 3 - 3x$

$\underset{8,2}{n} = -1 + 3x - \dfrac{3y}{C}$

$\underset{9,2}{n} = 3x - \dfrac{3y}{C}$

$\underset{9,3}{n} = -1 + \dfrac{3y}{C}$

Substituting the vabove shape functions in (3.8), (3.9) & (3.14) w.r.t each element and integrating over the respective triangular domain we obtain the element in the form (3.8).The 3x3 matrix equations are assembled using connectivity conditions to obtain a 8x8 matrix equations for the global nodes ψ_p,θ_p and ϕ_p.

The global matrix equation for θ is:

$$A_3 X_3 = B_3 \tag{4.1}$$

The global matrix equation for ϕ is:

$$A_4 X_4 = B_4 \tag{4.2}$$

The global matrix equation for ψ is:

$$A_5 X_5 = B_5 \tag{4.3}$$

Where:

$$A_3 = \begin{pmatrix} -1 & a_{12} & a_{13} & 0 & 0 & 0 & 0 & 0 & 0 & 0 & 0 \\ 0 & a_{22} & a_{23} & 0 & 0 & 0 & 0 & 0 & 0 & 0 & 0 \\ 0 & a_{32} & a_{33} & a_{34} & a_{35} & 0 & 0 & 0 & 0 & 0 & 0 \\ 0 & 0 & a_{44} & a_{44} & a_{45} & 0 & 0 & 0 & 0 & 0 & 0 \\ 0 & 0 & a_{53} & a_{54} & a_{55} & a_{56} & a_{57} & 0 & 0 & 0 & 0 \\ 0 & 0 & 0 & 0 & a_{65} & a_{66} & a_{67} & 0 & 0 & 0 & 0 \\ 0 & 0 & 0 & 0 & a_{75} & a_{76} & a_{77} & a_{78} & a_{79} & 0 & 0 \\ 0 & 0 & 0 & 0 & 0 & 0 & a_{87} & a_{88} & a_{89} & 0 & 0 \\ 0 & 0 & 0 & 0 & 0 & 0 & a_{97} & a_{98} & a_{99} & a_{910} & 0 \\ 0 & 0 & 0 & 0 & 0 & 0 & 0 & 0 & a_{109} & a_{1010} & 0 \\ 0 & 0 & 0 & 0 & 0 & 0 & 0 & 0 & a_{119} & a_{1110} & -1 \end{pmatrix}$$

$$A_4 = \begin{pmatrix} 1 & b_{1,2} & b_{1,3} & 0 & 0 & 0 & 0 & 0 & 0 & 0 & 0 \\ 0 & b_{2,2} & b_{2,3} & 0 & 0 & 0 & 0 & 0 & 0 & 0 & 0 \\ 0 & b_{3,2} & b_{3,3} & b_{3,4} & b_{3,5} & 0 & 0 & 0 & 0 & 0 & 0 \\ 0 & 0 & b_{4,3} & b_{4,4} & b_{4,5} & 0 & 0 & 0 & 0 & 0 & 0 \\ 0 & 0 & b_{5,3} & b_{5,4} & b_{5,5} & b_{5,6} & b_{5,7} & 0 & 0 & 0 & 0 \\ 0 & 0 & 0 & 0 & b_{6,5} & b_{6,6} & b_{6,7} & 0 & 0 & 0 & 0 \\ 0 & 0 & 0 & 0 & b_{7,5} & b_{7,6} & b_{7,7} & b_{7,8} & b_{7,9} & 0 & 0 \\ 0 & 0 & 0 & 0 & 0 & 0 & b_{8,7} & b_{8,8} & b_{8,9} & 0 & 0 \\ 0 & 0 & 0 & 0 & 0 & 0 & b_{9,7} & b_{9,8} & b_{9,9} & b_{9,10} & 0 \\ 0 & 0 & 0 & 0 & 0 & 0 & 0 & 0 & b_{10,9} & b_{10,10} & 0 \\ 0 & 0 & 0 & 0 & 0 & 0 & 0 & 0 & b_{11,9} & b_{11,10} & b_{11,11} \end{pmatrix}$$

$$A_5 = \begin{pmatrix} -1 & 0 & 0 & 0 & 0 & 0 & 0 & 0 & 0 & 0 \\ 0 & -1 & 0 & 0 & 0 & 0 & 0 & 0 & 0 & 0 \\ 0 & 0 & -1 & 0 & 0 & 0 & 0 & 0 & 0 & 0 \\ 0 & 0 & 0 & -1 & 0 & 0 & 0 & 0 & 0 & 0 \\ 0 & 0 & 0 & 0 & -1 & 0 & 0 & 0 & 0 & 0 \\ 0 & 0 & 0 & 0 & 0 & 0 & 0 & 0 & 0 & 0 \\ 0 & 0 & 0 & 0 & 0 & 0 & 0 & 0 & 0 & 0 \\ 0 & 0 & 0 & 0 & 0 & 0 & 0 & 0 & 0 & 0 \\ 0 & 0 & 0 & 0 & 0 & 0 & 0 & 0 & -1 & 0 \\ 0 & 0 & 0 & 0 & 0 & 0 & 0 & 0 & 0 & -1 \end{pmatrix}$$

$$X_3 = \begin{bmatrix} \theta_1 \\ \theta_2 \\ \theta_3 \\ \theta_4 \\ \theta_5 \\ \theta_6 \\ \theta_7 \\ \theta_8 \\ \theta_9 \\ \theta_{10} \\ \theta_{11} \end{bmatrix} \qquad X_4 = \begin{bmatrix} C_1 \\ C_2 \\ C_3 \\ C_4 \\ C_5 \\ C_6 \\ C_7 \\ C_8 \\ C_9 \\ C_{10} \\ C_{11} \end{bmatrix} \qquad X_5 = \begin{bmatrix} u_1 \\ u_2 \\ u_3 \\ u_4 \\ u_5 \\ u_6 \\ u_7 \\ u_8 \\ u_9 \\ u_{10} \\ u_{11} \end{bmatrix}$$

$$B_3 = \begin{pmatrix} ar_1 \\ ar_2 \\ ar_3 \\ ar_4 \\ ar_5 \\ ar_6 \\ ar_7 \\ ar_8 \\ ar_9 \\ ar_{10} \\ ar_{11} \end{pmatrix} \qquad B_4 = \begin{pmatrix} br_1 \\ br_2 \\ br_3 \\ br_4 \\ br_5 \\ br_6 \\ br_7 \\ br_8 \\ br_9 \\ br_{10} \\ br_{11} \end{pmatrix} \qquad B_5 = \begin{pmatrix} cr_1 \\ cr_2 \\ cr_3 \\ cr_4 \\ cr_5 \\ cr_6 \\ cr_7 \\ cr_8 \\ cr_9 \\ cr_{10} \\ cr_{11} \end{pmatrix}$$

The global matrix equations are coupled and are solved under the following iterative procedures. At the beginning of the first iteration the values of (ψ_i) are taken to be zero and the global equations (4.1) & (4.2) are solved for the nodal values of θ and ϕ.These nodal values (θi) and (ϕi) obtained are then used to solve the global equation (4.3) to obtain (ψ_i). In the second iteration these (ψ_i) values are obtained are used in (4.1) & (4.2) to calculate (θi) and (ϕi) and vice versa. The three equations are thus solved under iteration process until two consecutive iterations differ by a pre-assigned percentage.

The domain consists three horizontal levels and the solution for Ψ & θ at each level may be expressed in terms of the nodal values as follows,

In the horizontal strip: $0 \le y \le \frac{c}{3}$

$$\Psi = (\Psi_1 N^1_1 + \Psi_2 N^1_2 + \Psi_7 N^1_7)\, H(1-\tau_1)$$

$$= \Psi_1 (1-4x) + \Psi_2 4\left(x-\frac{y}{c}\right) + \Psi_7 \left(\frac{4y}{c}\right.\ (1-\tau_1) \qquad \left(0 \le x \le \frac{1}{3}\right)$$

$$\Psi = (\Psi_2 N^3_2 + \Psi_3 N^3_3 + \Psi_6 N^3_6)\, H(1-\tau_2)$$

$$+ (\Psi_2 N^2_2 + \Psi_7 N^2_7 + \Psi_6 N^2_6) H(1-\tau_3) \qquad \left(\frac{1}{3} \le x \le \frac{1}{3}\right)$$

$=(\Psi_2 2(1-2x) + \Psi_3\,(4x-\frac{4y}{c}-1)+ \Psi_6\,(\frac{4y}{c}))H(1-\tau_2)$

$+(\Psi_2\,(1-\frac{4y}{c})+ \Psi_7\,(1+\frac{4y}{c}-4x)+ \Psi_6\,(4x-1))H(1-\tau_3)$

$\Psi =(\Psi_3 N^5_3+ \Psi_4 N^5_4+ \Psi_5 N^5_5)\, H(1-\tau_3)$

$+ (\Psi_3 N^4_3+ \Psi_5 N^4_5+ \Psi_6 N^4_6)H(1-\tau_4)$ $\qquad (\frac{2}{3} \le x \le 1)$

$=(\Psi_3\,(3-4x) + \Psi_4 2(2x-\frac{2y}{c}-1)+ \Psi_6\,(\frac{4y}{c}-4x+3))H(1-\tau_3)$

$+ \Psi_3\,(1-\frac{4y}{c})+ \Psi_5\,(4x-3)+ \Psi_6\,(\frac{4y}{c}))H(1-\tau_4)$

Along the strip $\frac{c}{3} \le y \le \frac{2c}{3}$

$\Psi =(\Psi_7 N^6_7+ \Psi_6 N^6_6+ \Psi_8 N^6_8)\, H(1-\tau_2)$ $\qquad (\frac{1}{3} \le x \le 1)$

$+(\Psi_6 N^7_6+ \Psi_9 N^7_9+ \Psi_8 N^7_8)\, H(1-\tau_3)+(\Psi_6 N^8_6+ \Psi_5 N^8_5+ \Psi_9 N^8_9)\, H(1-\tau_4)$

$\Psi =(\Psi_7\, 2(1-2x) + \Psi_6\,(4x-3)+ \Psi_8\,(\frac{4y}{c}-1))H(1-\tau_3)$

$+ \Psi_6\,(2(1-\frac{2y}{c})+ \Psi_9\,(\frac{4y}{c}-1)+ \Psi_8\,(1+\frac{4y}{c}-4x))H(1-\tau_4)$

$+ \Psi_6\,(4(1-x)+ \Psi_5\,(4x-\frac{4y}{c}-1)+ \Psi_9 2(\frac{2y}{c}-1))H(1-\tau_5)$

Along the strip $\frac{2c}{3} \le y \le 1$

$\Psi =(\Psi_8 N^9_8+ \Psi_9 N^9_9+ \Psi_{10} N^9_{10})\, H(1-\tau_6)$ $\qquad (\frac{2}{3} \le x \le 1)$

$= \Psi_8\,(4(1-x)+ \Psi_9 4(x-\frac{y}{c})+ \Psi_{10} 2(\frac{4y}{c}-3))H(1-\tau_6)$

where $\tau_1= 4x$, $\tau_2 = 2x$, $\tau_3 = \frac{4x}{3}$,

$\tau_4= 4(x-\frac{y}{c})$, $\tau_5= 2(x-\frac{y}{c})$, $\tau_6 = \frac{4}{3}(x-\frac{y}{c})$

and H represents the Heaviside function.

The expressions for θ are:

In the horizontal strip $0 \le y \le \frac{c}{3}$

$\theta = [\theta_1(1-4x)+ \theta_2\, 4(x-\frac{y}{c})+ \theta_7\,(\frac{4y}{c}))\, H(1-\tau_1)$ $\qquad (0 \le x \le \frac{1}{3})$

$\theta = (\theta_2(2(1-2x)+ \theta_3\,(4x-\frac{4y}{c}-1)+ \theta_6(\frac{4y}{c}))\, H(1-\tau_2)$

$+ \theta_2(1-\frac{4y}{c})+ \theta_7(1+\frac{4y}{c}-4x)+ \theta_6(4x-1))H(1-\tau_3)$ $\qquad (\frac{1}{3} \le x \le \frac{2}{3})$

$$\theta = \theta_3(3-4x) + 2\,\theta_4(2x-\frac{2y}{c}-1) + \theta_6(\frac{4y}{c}-4x+3)\,H(1-\tau_3)$$

$$+(\theta_3(1-\frac{4y}{c}) + \theta_5(4x-3) + \theta_6(\frac{4y}{c}))\,H(1-\tau_4) \qquad (\frac{2}{3} \le x \le 1)$$

Along the strip $\frac{c}{3} \le y \le \frac{2c}{3}$

$$\theta = (\theta_7(2(1-2x) + \theta_6(4x-3) + \theta_8(\frac{4y}{c}-1))\,H(1-\tau_3) \qquad (\frac{1}{3} \le x \le \frac{2}{3})$$

$$+(\theta_6(2(1-\frac{2y}{c}) + \theta_9(\frac{4y}{c}-1) + \theta_8(1+\frac{4y}{c}-4x))\,H(1-\tau_4)$$

$$+(\theta_6(4(1-x) + \theta_5(4x-\frac{4y}{c}-1) + \theta_9\,2(\frac{4y}{c}-1))\,H(1-\tau_5)$$

Along the strip $\frac{2c}{3} \le y \le 1$

$$\theta = (\theta_8 4(1-x) + \theta_9 4(x-\frac{y}{c}) + \theta_{10}(\frac{4y}{c}-3)\,H(1-\tau_6) \qquad (\frac{2}{3} \le x \le 1)$$

The expressions for ϕ are:

$$\phi = [\phi_1(1-4x) + \phi_2\,4(x-\frac{y}{c}) + \phi_7\,(\frac{4y}{c}))\,H(1-\tau_1) \qquad (0 \le x \le \frac{1}{3})$$

$$\phi = (\phi_2(2(1-2x) + \phi_3\,(4x-\frac{4y}{c}-1) + \phi_6(\frac{4y}{c}))\,H(1-\tau_2)$$

$$+\phi_2(1-\frac{4y}{c}) + \phi_7(1+\frac{4y}{c}-4x) + \phi_6(4x-1))H(1-\tau_3) \qquad (\frac{1}{3} \le x \le \frac{2}{3})$$

$$\phi = \phi_3(3-4x) + 2\,\phi_4(2x-\frac{2y}{c}-1) + \phi_6(\frac{4y}{c}-4x+3)\,H(1-\tau_3)$$

$$+(\phi_3(1-\frac{4y}{c}) + \phi_5(4x-3) + \phi_6(\frac{4y}{c}))\,H(1-\tau_4) \qquad (\frac{2}{3} \le x \le 1)$$

Along the strip $\frac{c}{3} \le y \le \frac{2c}{3}$

$$\phi = (\phi_7(2(1-2x) + \phi_6(4x-3) + \phi_8(\frac{4y}{c}-1))\,H(1-\tau_3) \qquad (\frac{1}{3} \le x \le \frac{2}{3})$$

$$+(\phi_6(2(1-\frac{2y}{c}) + \phi_9(\frac{4y}{c}-1) + \phi_8(1+\frac{4y}{c}-4x))\,H(1-\tau_4)$$

$$+(\phi_6(4(1-x) + \phi_5(4x-\frac{4y}{c}-1) + \phi_9\,2(\frac{4y}{c}-1))\,H(1-\tau_5)$$

Along the strip $\frac{2c}{3} \le y \le 1$

$$\phi = (\phi_8 4(1-x) + \phi_9 4(x-\frac{y}{c}) + \phi_{10}(\frac{4y}{c}-3)\,H(1-\tau_6) \qquad (\frac{2}{3} \le x \le 1)$$

The dimensionless Nusselt numbers(Nu) and Sherwood Numbers (Sh) on the non-insulated boundary walls of the rectangular duct are calculated using the formula:

$$\text{Nu} = \left(\frac{\partial\theta}{\partial x}\right)_{x=1} \text{ and } \text{Sh} = \left(\frac{\partial\phi}{\partial x}\right)_{x=1}$$

Nusselt Number on the side wall x=1in different regions are:

$Nu_1=2-4\theta_3 \quad (0 \le y \le h/3)$

$Nu_2=2-4\theta_5 \quad (h/3 \le y \le 2h/3)$

$Nu_3=2-4\theta_7 \quad (2h/3 \le y \le h)$

Sherwood Number on the side wall x=1 in different regions are:

$Sh_1=2-4\phi_3 \quad (0 \le y \le h/3)$

$Sh_2=2-4\phi_5 \quad (h/3 \le y \le 2h/3)$

$Sh_3=2-4\phi_7 \quad (2h/3 \le y \le h)$

5 DISCUSSION OF THE NUMERICAL RESULTS

In this analysis we investigate the effect of chemical reaction on the mixed convective heat and mass transfer flow of a viscous electrically conducting fluid through a porous medium n a rectangular cavity.

The non-dimensional temperature (θ) is shown in figs 1-32 at different horizontal and vertical levels with variations in Ra, α, Sc, N, N_1, Ec, k and M. Figs. 1-4 represents the temperature(θ) with Rayleigh number Ra at horizontal and vertical levels. It is found that the actual temperature depreciates with Ra $\le$ 2x10^2 and enhances at Ra $\ge$ 3x10^2 at all levels. An increase in |Ra| enhances the actual temperature at $y=\frac{2h}{3}$ and $x=\frac{2}{3}$ levels while it depreciates at $y=\frac{h}{3}$ and $x=\frac{1}{3}$ levels (figs. 1-4). Figs. 5-8 represents θ with heat source parameter α. At levels $x=\frac{1}{3}$, $y=\frac{h}{3}$ & $y=\frac{2h}{3}$ the actual temperature reduces with increase in the strength of the heat source and enhances with the strength of the heat sink. At $x=\frac{2}{3}$ level, the actual temperature enhances with $\alpha \le 4$ and for higher $\alpha \ge 6$, it reduces in the horizontal strip (0, 0.462) and enhances in the horizontal strip (0.528, 0.666) while an increase in $|\alpha| \le 4$, results in a depreciation in the region (0, 0.066) and enhances in the horizontal strip (0.132, 0.666) (fig. 8). Figs. 9-12 represent θ with Schmidt number Sc. It is found that an increase in Sc $\le$ 0.6, reduces the actual temperature at $y=\frac{2h}{3}$ level and enhances at $y=\frac{h}{3}$ level while it enhances with Sc = 1.3 and reduces with higher Sc = 2.01 at both the horizontal levels. At the vertical level $x=\frac{1}{3}$, it enhances with Sc $\le$ 1.3 and reduces with higher Sc $\ge$ 2.01. At the higher vertical level $x=\frac{2}{3}$, lesser the molecular diffusivity larger the actual temperature in the horizontal strip (0, 0.066) and lesser in the strip (0.132, 0.666).

For further lowering of the molecular diffusivity larger the temperature in the strip (0, 0.396) and lesser in the strip (0.462, 0.666) and for still lowering of the diffusivity lesser in the region (0, 0.396) and larger the actual temperature in the region (0.462, 0.666)(fig. 12). The variation of θ with buoyancy ratio N shows that when the molecular buoyancy force dominates over the thermal buoyancy force the actual temperature depreciates at all levels irrespective of the directions of the buoyancy forces (figs. 13-16). The variation of θ with radiation parameter N_1 is shown in figs. 17-20. It is found that higher the radiative heat flux lesser the actual temperature, for further higher flux, larger the actual temperature and for still higher radiative heat flux lesser the temperature at all horizontal levels and vertical level $x=\frac{1}{3}$. At the higher vertical level $x=\frac{2}{3}$, an increase in $N_1 \le 0.03$, leads to a depreciation in the actual temperature, for higher $N_1 \ge 0.05$, larger in the horizontal strip (0, 0.264) and lesser in the region (0.33, 0.666) and for still higher N_1 = 0.07, the actual temperature enhances in the region except in a narrow region adjacent to y = 0(fig. 20). The influence of dissipative effect on θ is shown in figs. 21-24 at different levels. From figs. 21&23 it follows that the actual temperature reduces with Ec ≤ 0.005 and enhances with higher Ec ≥ 0.007 at $y = \frac{2h}{3}$ level and $x = \frac{1}{3}$ level. At the horizontal level it depreciates with lower and higher values of Ec and depreciates with intermediate value Ec = 0.005 while at the higher vertical level $x = \frac{2}{3}$, the actual temperature fluctuates with Ec (fig. 24). The influence of chemical reaction on θ is shown in figs. 25-28. It if found that the actual temperature depreciates in the degenerating chemical reaction case at all horizontal and vertical levels while in the generating chemical reaction case, it reduces with |k| ≤ 1.5 and enhances with |k| ≥ 2.5 at $y = \frac{h}{3}$, $y = \frac{2h}{3}$ and $x = \frac{1}{3}$ levels. At te higher vertical $x = \frac{2}{3}$, an increase in |k| ≤ 1.5, depreciates the actual temperature while for higher |k| ≥ 2.5, it depreciates in the horizontal strip (0, 0.264) and enhances in the region (0.33, 0.666) (fig. 28). Figs. 29-32 represent θ wit Hartman number M. It is found that higher the Lorentz force lesser the actual temperature at $y = \frac{h}{3}$, $y = \frac{2h}{3}$ and $x = \frac{1}{3}$ levels and for further higher Lorentz force lesser at $y = \frac{2h}{3}$ level and larger at $y = \frac{h}{3}$ and $x = \frac{1}{3}$ levels. At $x = \frac{2}{3}$ level, the actual temperature reduces θ with M ≤ 10 in the region (0, 0.264) and enhances in the region (0.33, 0.666) and for higher M ≥ 15, lesser the actual temperature in the entire flow region (fig. 32).

The non-dimensional concentration (C) is show in figs. 33-64 at different horizontal and vertical levels. Figs 33-36 represent the concentration with Rayleigh number Ra. It is found that at the levels $y = \frac{h}{3}$ and $x = \frac{1}{3}$, the actual concentration enhances with Ra ≤ $2x10^2$ and depreciates with Ra ≥ $3x10^2$ while it reduces with increase n |Ra| (<0)(figs. 34&35). At the higher levels $y = \frac{2h}{3}$ and $x = \frac{2}{3}$, the actual concentration reduces with Ra ≤ $2x10^2$ and enhances with Ra ≥ $3x10^2$ while it enhances with |Ra| at both the levels (figs. 33 & 36). The variation of C with heat source parameter α shows that at the horizontal levels the actual concentration enhances with increase in the strength of the heat source/sink (figs. 37&38).At the vertical level $x = \frac{1}{3}$ the actual concentration enhances with increase in α ≤ 4 and depreciates with α ≥ 6,while it enhances with increase in the strength of heat source (fig. 39). At the higher vertical level $x = \frac{2}{3}$ an increase in the strength of heat source enhances the concentration in the horizontal strip (0, 0.33) and depreciates in the region (0.396, 0.666) while it enhances with increase in the strength of heat sink (fig. 40). The variation of C with buoyancy ratio N shows that at the horizontal levels $y = \frac{h}{3}$ and $y = \frac{2h}{3}$ and vertical level $x = \frac{1}{3}$ the actual concentration depreciates when the buoyancy forces act in the same direction and enhances when forces act in opposite direction (figs. 45-47). At $x = \frac{2}{3}$ level the actual concentration depreciates with N>0 in the horizontal strip (0, 0.33) and enhances in the remaining region and a reversed effect is observed in the actual concentration with increase in |N|(fig. 48). The variation of C with Schmidt number Sc shows that at $y = \frac{h}{3}$ and $x = \frac{1}{3}$ levels lesser the molecular diffusivity larger the actual concentration and for further lowering of the diffusivity smaller the concentration (figs. 42-43). At higher horizontal level $y = \frac{2h}{3}$ the actual concentration depreciates with Sc ≤ 1.3 and enhances with higher Sc ≥ 2.01 (fig. 41). At $x = \frac{2}{3}$ level for smaller and higher values of Sc the actual concentration enhances in the region (0, 0.33) and depreciates in the region (0.396, 0.666) and for Sc = 1.3, it depreciates in the region (0, 0.033) and enhances in the remaining region.

The variation of C with radiation parameter N_1 in shown figs. 49-52.It is found that at both the horizontal levels the actual concentration depreciates with radiation parameter $N_1 \leq 0.03$ and enhances with higher $N_1 \geq 0.07$ (figs. 49&50). At $x = \frac{1}{3}$ level the actual concentration enhances with $N_1 = \leq 0.03$ and depreciates with $N_1 \geq 0.05$. From fig 52 we find that for smaller and moderate values of N_1 the actual concentration reduces in the region (0, 0.264) and enhances in the region (0.33, 0.666) while for intermediate value of $N_1 = 0.05$ it depreciates in the horizontal strip (0, 0.33) and enhances in the region (0.396, 0.666). The variation of C with Eckert number Ec is shown in figs. 53-56 at different levels. It is found from figs.53&54 that the actual concentration enhances with lower and higher values of Ec and depreciates with intermediate value of higher values of Ec and depreciates with intermediate value of Ec = 0.005. At $x = \frac{1}{3}$ level the actual concentration depreciates with Ec $\leq$ 0.005 and enhances with Ec $\geq$ 0.007 (fig. 55). At higher vertical level $x = \frac{2}{3}$ the actual concentration enhances with Ec $\leq$ 0.005 in the region (0, 0.132) and depreciates in the remaining region and for Ec $\leq$ 0.007 we notice an enhancement in the actual concentration everywhere in the region (fig. 56).The influence of the chemical reaction on C is shown in figs. 57-60 at different levels. At $y = \frac{2h}{3}$, the actual concentration depreciates in the degenerating chemical reaction case and enhances in the generating chemical reaction case. At $y = \frac{h}{3}$ and $x = \frac{1}{3}$ levels the actual concentration depreciates with increase in k $\leq$ 1.5 and enhances with k $\geq$ 2.5 at both the levels, while an increase in |k| $\leq$ 1.5 enhances the concentration at $y = \frac{h}{3}$ level and depreciates at $x = \frac{1}{3}$ level, and for higher |k| $\geq$ 2.5 it depreciates at $y = \frac{h}{3}$ level and enhances at $x = \frac{1}{3}$ level (figs. 58&59). At higher vertical level $x = \frac{2}{3}$ the actual concentration experiences an enhancement with k>0 and for |k| $\leq$ 1.5 we notice an enhancement in the region (0, 0.264) and depreciation in the region (0.33, 0.666) and for higher |k| $\geq$ 2.5 it depreciates in the region (0, 0.264) and enhances in the remaining region (fig. 60).The variation of C with Hartman number M is shown in figs. 61-64 at different levels. It is found that at $y = \frac{h}{3}$ level and $x = \frac{1}{3}$ level higher the Lorentz force lesser the actual concentration (figs. 62-63). At $y = \frac{2h}{3}$ level lesser the Lorentz force larger the actual concentration and for further higher the Lorentz force lesser the actual concentration (fig. 61). At $x = \frac{2}{3}$ level the actual concentration enhances in the region (0, 0.264) and depreciates in the region (0.33, 0.666) with M $\leq$ 10 and for higher M $\geq$ 15 and for higher M $\geq$ 15 we notice a reversed effect in the behavior of actual concentration (fig. 64).

The rate of heat transfer on the side wall x = 1 is evaluated for different values of Ra, α, Sc, N, N_1, Ec, k, and M and are presented in tables 1-3. The variation of Nu with Rayleigh number Ra shows that the Nusselt number enhances with increase in Ra in all the quadrants while for an increase in |Ra|, Nu depreciates in the lower quadrant and enhances in the middle and uppermost quadrants. An increase in the strength of the heat source enhances Nu in the lower and middle quadrants and reduces in the upper quadrant while the strength of the heat sink reduces Nu in the first quadrant and reduces it in the middle and upper quadrants. Lesser the molecular diffusivity larger the rate of heat transfer in all the three quadrants (table.1). When the molecular buoyancy force dominates over the thermal buoyancy force the rate of heat transfer enhances when the buoyancy forces act in the same direction while for the forces acting in opposite direction, it enhances in the lower and middle quadrants and reduces in the upper quadrant. An increase in the radiation parameter N_1 leads an enhancement in |Nu| in all the three quadrants. The variation of Nu with Ec shows that higher the dissipative heat larger |Nu| in the lower and middle quadrants and smaller in the upper quadrant (table. 2). From table. 3 we find that higher the Lorentz force larger Nu in all the quadrants. With respect to the chemical reaction parameter k, we find that the rate of heat transfer enhances in the lower and middle quadrants and reduces in the upper quadrant in the degenerating chemical reaction case while it enhances in the generating chemical reaction case in all the three quadrants (table. 3).

The rate of mass transfer (Sh) at x = 1 is shown in tables 4-6 for different variation. From table.4 we find that the rate of mass transfer enhances n the lower and middle quadrants and reduces in the upper quadrant with increase in Ra while it reduces with |Ra| in all the three quadrants. An increase in α>0 reduces with Sh in all the quadrants while for $|\alpha|$ (<0), it reduces in the middle quadrant. Lesser the molecular diffusivity smaller |Sh| in the lower and middle quadrants and enhances in the upper quadrant(table. 4). The variation of Sh with buoyancy ratio N shows that |Sh| enhances with N>0 and for |N| (<0), Sh depreciates in the lower and middle quadrants and enhances in the upper quadrant. An increase in the radiation parameter $N_1 \leq 0.05$ enhances Sh in the middle and upper quadrants and reduces with higher $N_1 \geq 0.07$ while the rate of mass transfer in the first quadrant reduces with $N_1 \leq 0.05$ and enhances with $N_1 \geq 0.07$. Also higher the dissipative heat larger Sh and for higher dissipative heat lesser Sh in all the three quadrants (table. 5). With respect to Hartmann number M we find that the higher the Lorentz force larger Sh in all the quadrants. An increase in the chemical reaction parameter k>0 reduces Sh in the lower and middle quadrants and reduces in the upper quadrant while an increase in |k| (<0) $\leq$ 1.5, reduces Sh in the first quadrant and enhances in the middle and upper quadrants while for $|k| \geq 2.5$, we find an enhancement in Sh in the first quadrant and depreciates in the other two quadrants (table. 6).

6 FIGURES

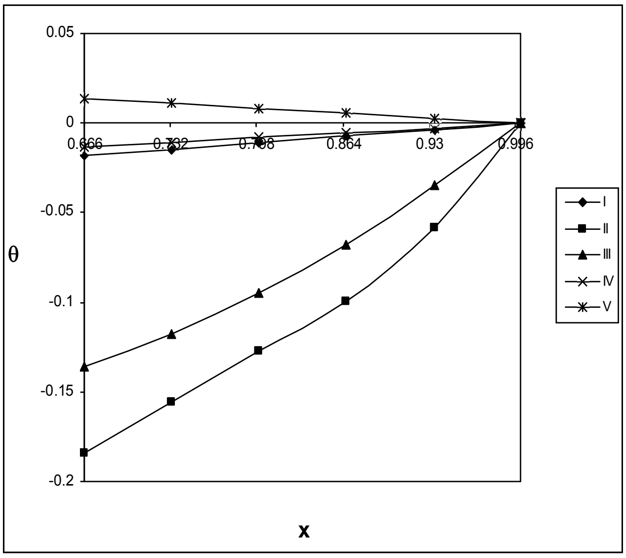

Fig. 1. Variation of θ ***with R at*** $y = \frac{2h}{3}$ ***level***

	I	II	III	IV	V
R	100	200	300	-100	-200

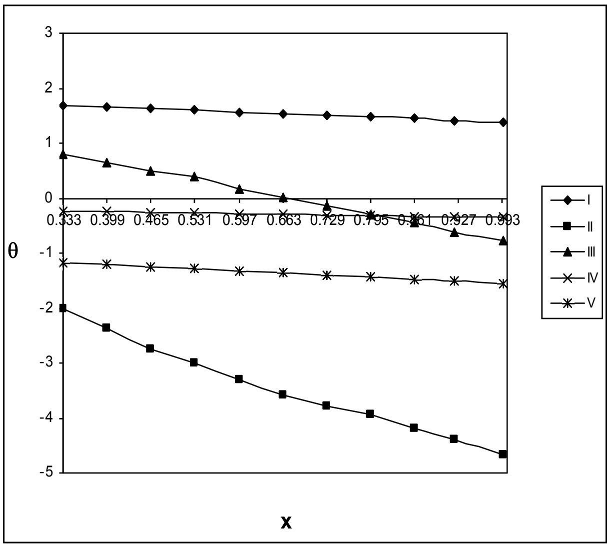

Fig. 2. Variation of θ ***with R at*** $y = \frac{h}{3}$ ***level***

	I	II	III	IV	V
R	100	200	300	-100	-200

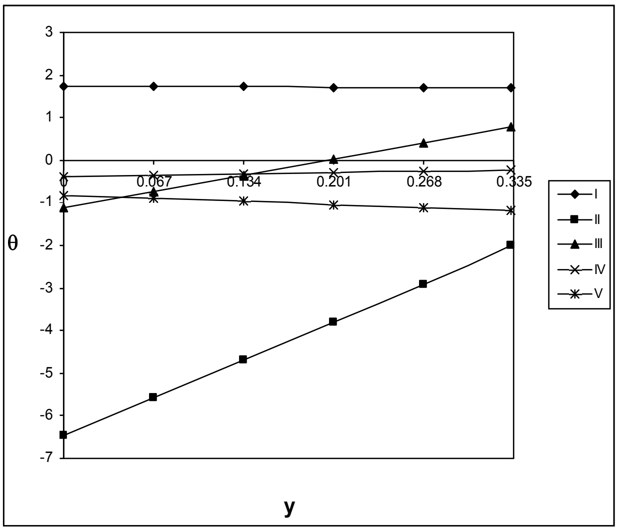

Fig. 3. Variation of θ with x at $x=\dfrac{2}{3}$ *level*

	I	II	III	IV	V
R	100	200	300	-100	-200

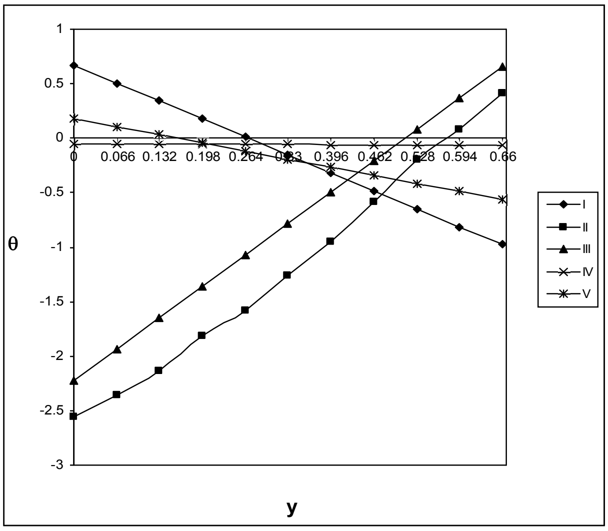

Fig. 4. Variation of θ with x at $x=\dfrac{1}{3}$ *level*

	I	II	III	IV	V
R	100	200	300	-100	-200

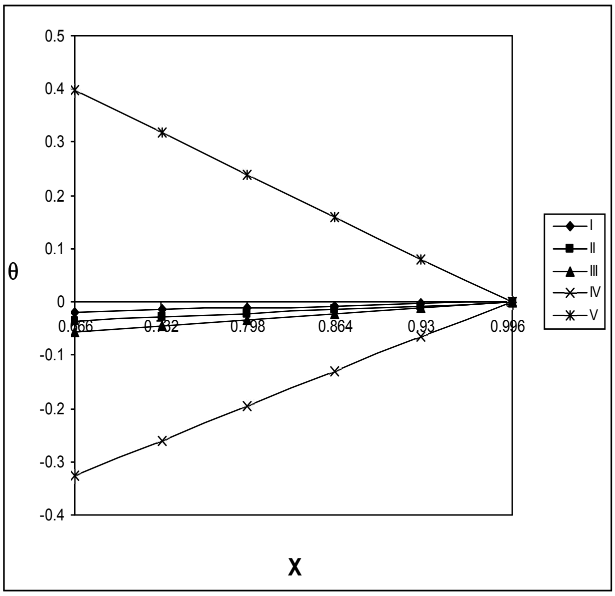

Fig. 5. Variation of θ with α at $y=\dfrac{2h}{3}$ *level*

	I	II	III	IV	V
α	2	4	6	-2	-4

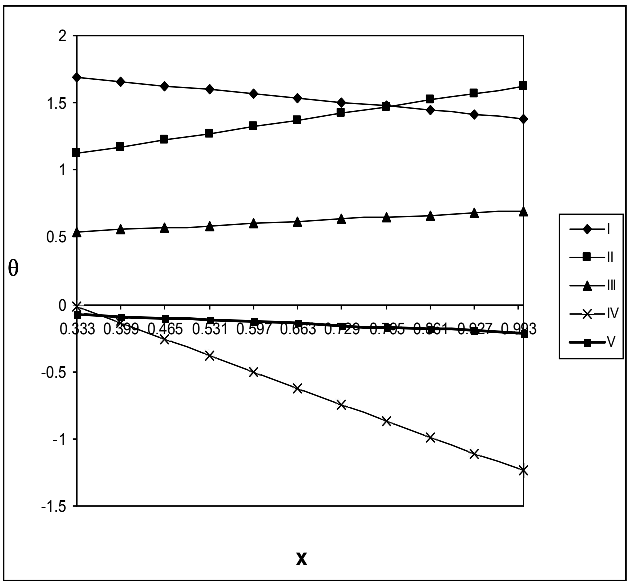

Fig. 6. Variation of θ with α at $y=\dfrac{h}{3}$ *level*

	I	II	III	IV	V
α	2	4	6	-2	-4

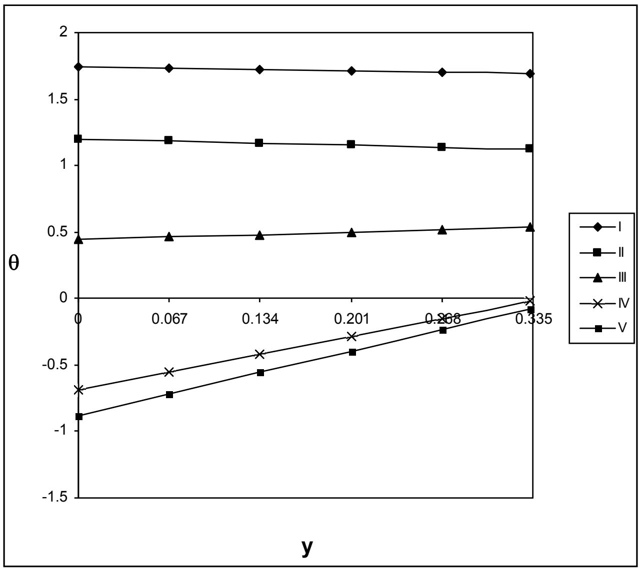

Fig. 7. Variation of θ with α at $x=\frac{1}{3}$ level

	I	II	III	IV	V
α	2	4	6	-2	-4

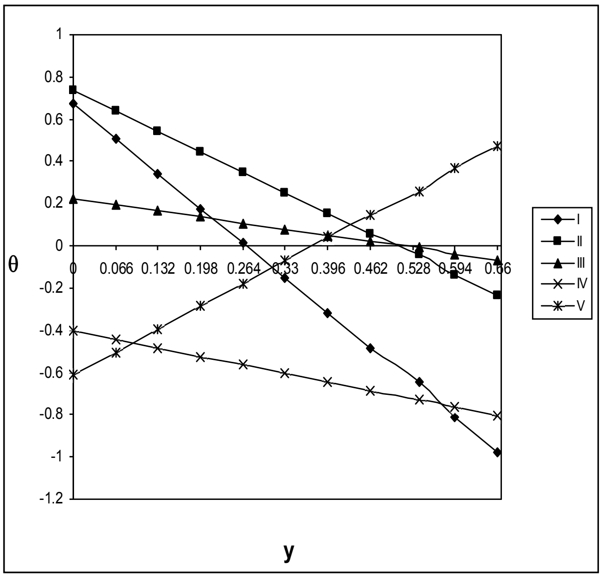

Fig. 8. Variation of θ with α at $x=\frac{2}{3}$ level

	I	II	III	IV	V
α	2	4	6	-2	-4

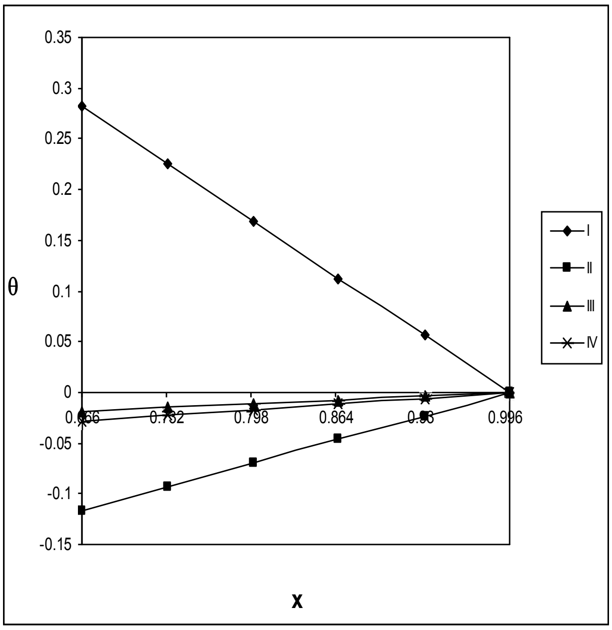

Fig. 9. Variation of θ with Sc at $y=\frac{2h}{3}$ level

	I	II	III	IV
Sc	0.24	0.6	1.3	2.01

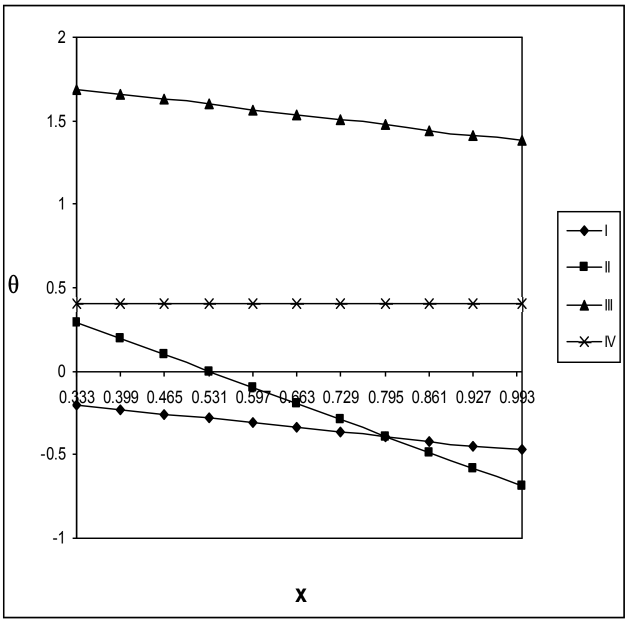

Fig. 10. Variation of θ with Sc at $y=\frac{h}{3}$ level

	I	II	III	IV
Sc	0.24	0.6	1.3	2.01

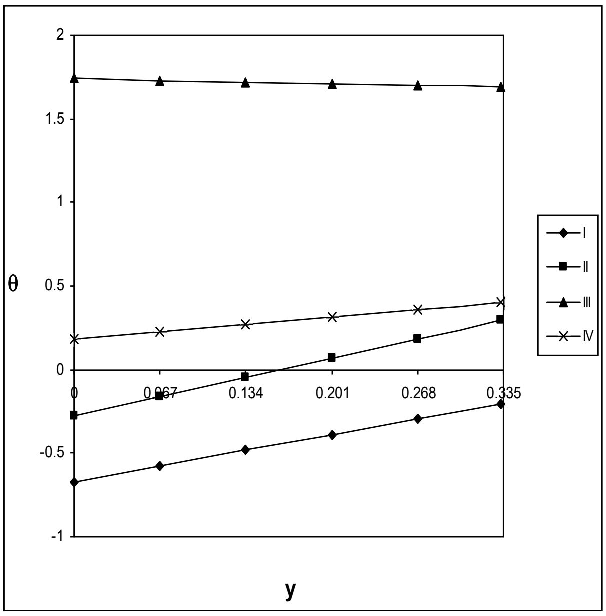

Fig. 11. Variation of θ with Sc at $x = \frac{1}{3}$ *level*

	I	II	III	IV
Sc	0.24	0.6	1.3	2.01

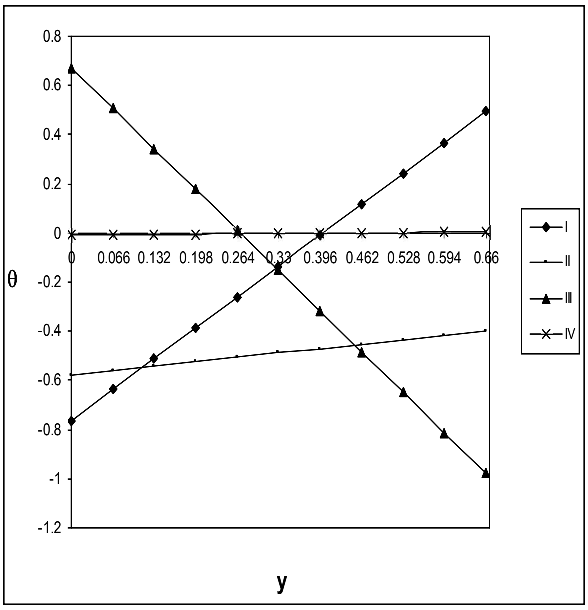

Fig. 12. Variation of θ with Sc at $x = \frac{2}{3}$ *level*

	I	II	III	IV
Sc	0.24	0.6	1.3	2.01

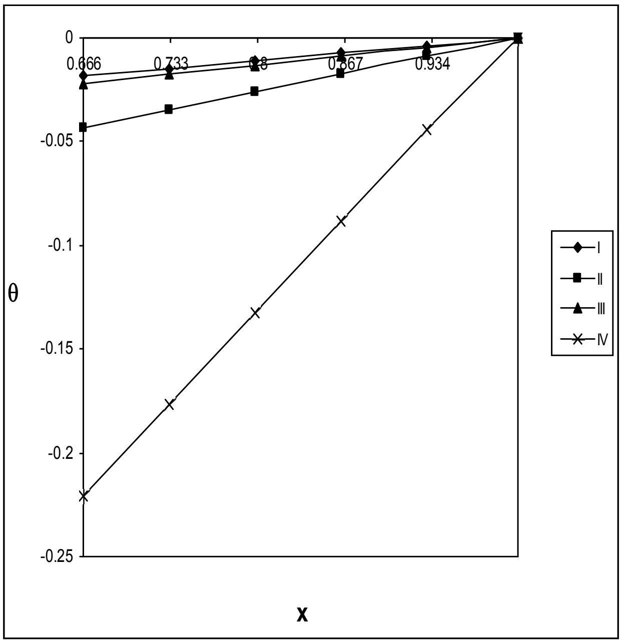

Fig. 13. Variation of θ with N at $y = \frac{2h}{3}$ *level*

	I	II	III	IV
N	1	2	-0.5	-0.8

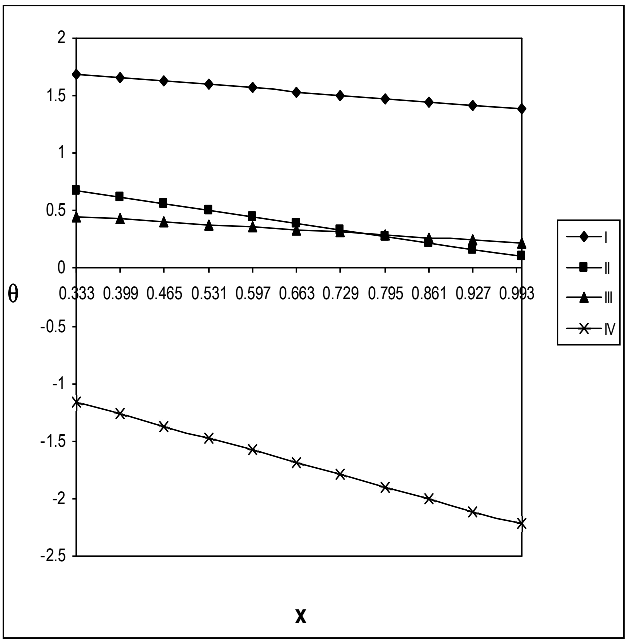

Fig. 14. Variation of θ with N at $y = \frac{h}{3}$ *level*

	I	II	III	IV
N	1	2	-0.5	-0.8

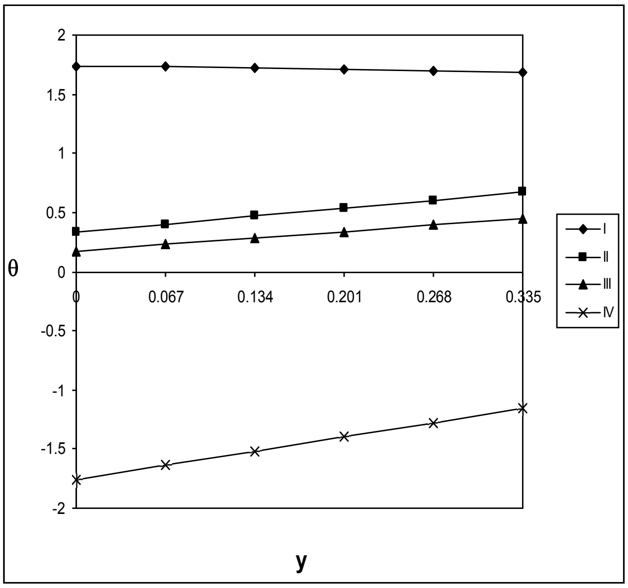

Fig. 15. Variation of θ with N at $x=\frac{1}{3}$ level

	I	II	III	IV
N	1	2	-0.5	-0.8

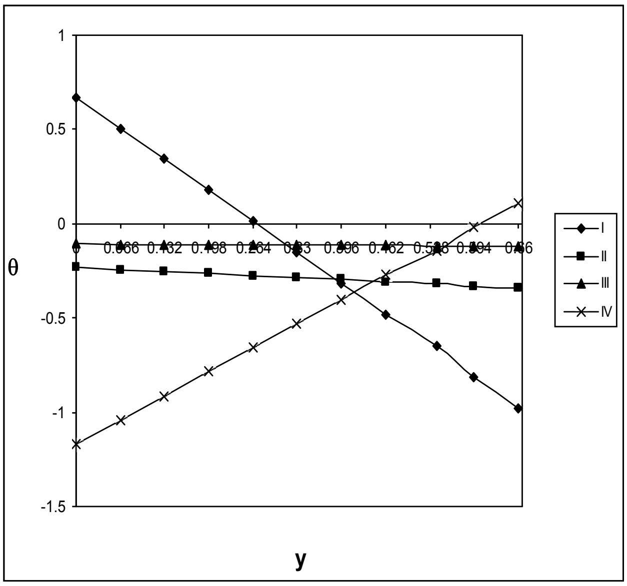

Fig. 16. Variation of θ with N at $x=\frac{2}{3}$ level

	I	II	III	IV
N	1	2	-0.5	-0.8

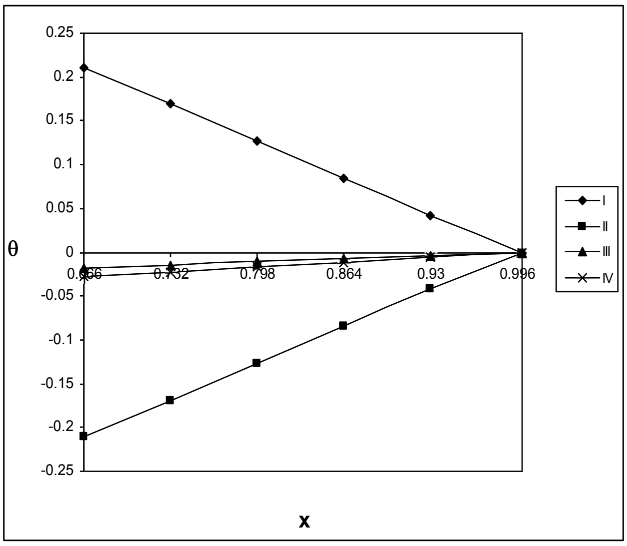

Fig. 17. Variation of θ with N_1 at $y=\frac{2h}{3}$ level

	I	II	III	IV
N_1	0.01	0.03	0.05	0.07

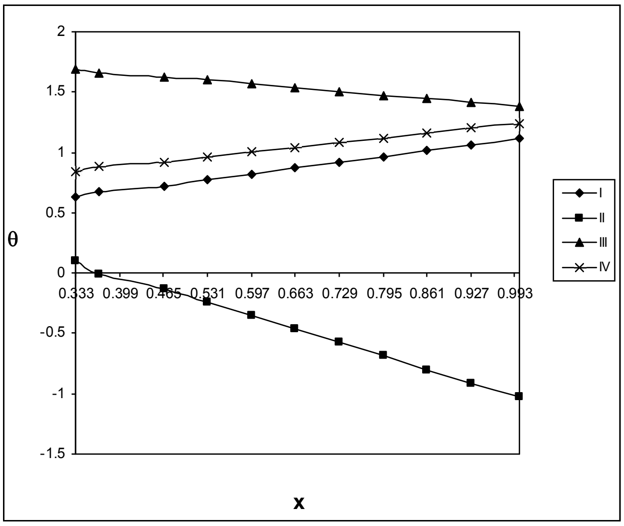

Fig. 18. Variation of θ with N_1 at $y=\frac{h}{3}$ level

	I	II	III	IV
N_1	0.01	0.03	0.05	0.07

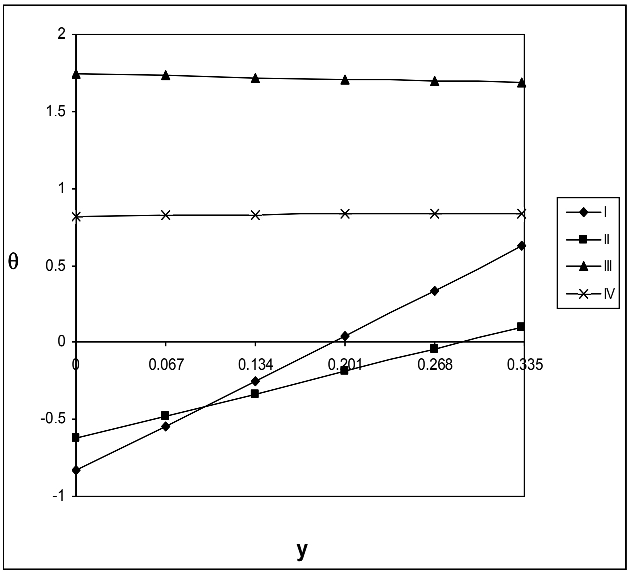

Fig. 19. Variation of θ with N_1 at $x = \frac{1}{3}$ level

	I	II	III	IV
N_1	0.01	0.03	0.05	0.07

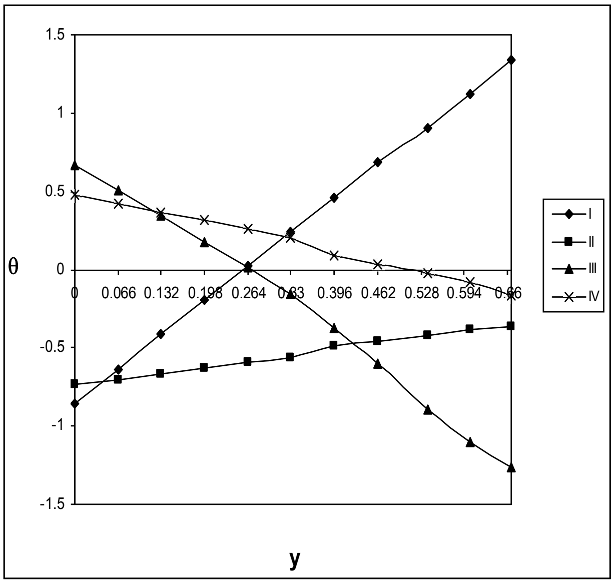

Fig. 20. Variation of θ with N_1 at $x = \frac{2}{3}$ level

	I	II	III	IV
N_1	0.01	0.03	0.05	0.07

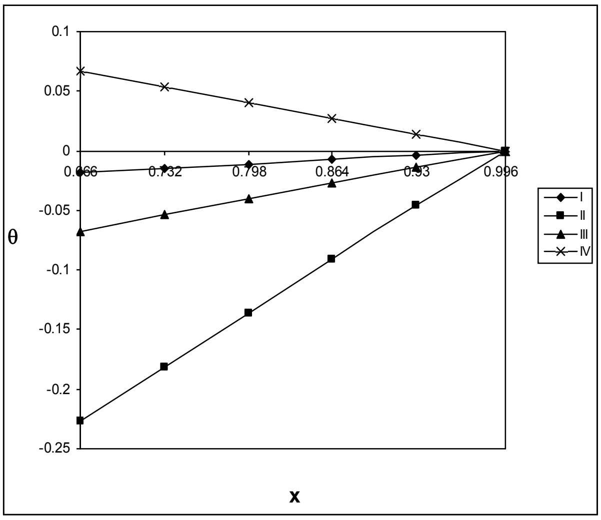

Fig. 21. Variation of θ with Ec at $y = \frac{2h}{3}$ level

	I	II	III	IV
Ec	0.001	0.003	0.005	0.007

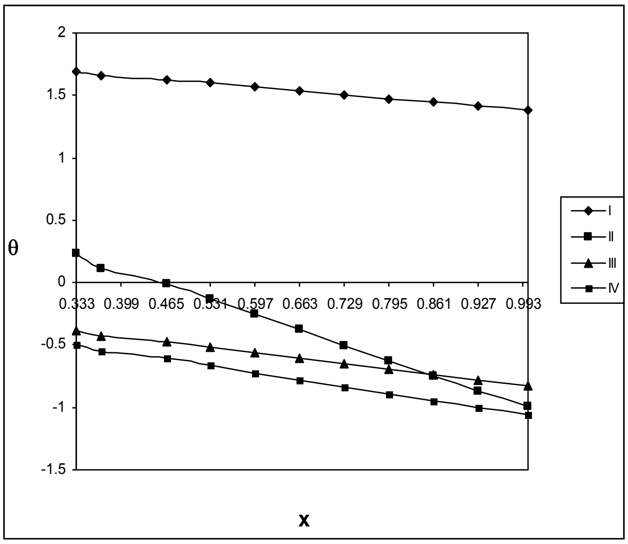

Fig. 22. Variation of θ with Ec at $y = \frac{h}{3}$ level

	I	II	III	IV
Ec	0.001	0.003	0.005	0.007

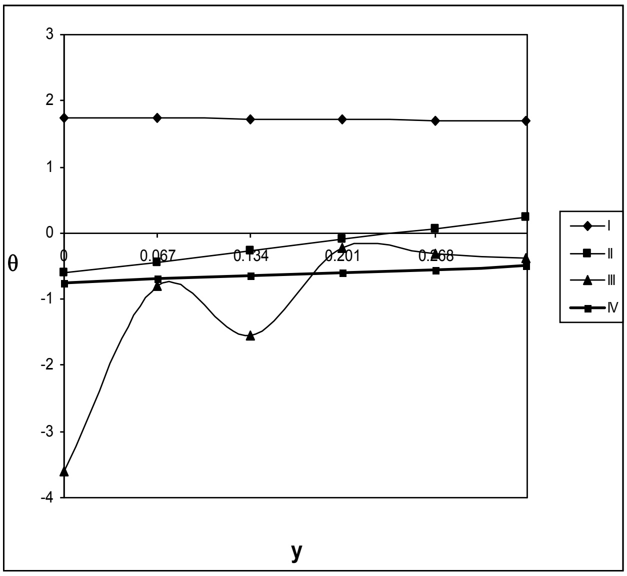

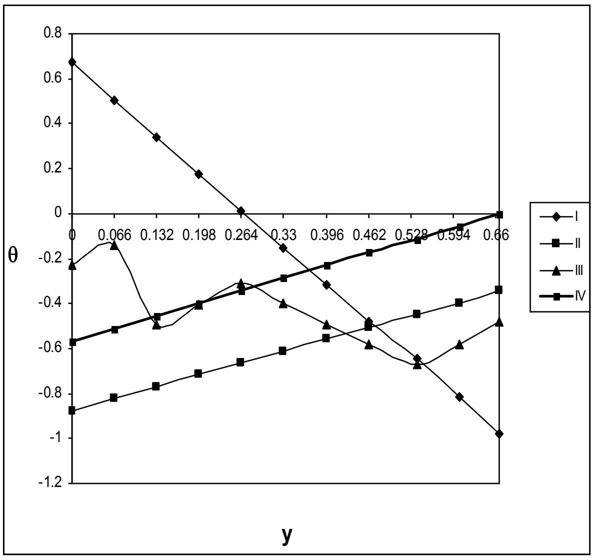

Fig. 23. Variation of* θ *with Ec at* $x=\frac{1}{3}$ *level

	I	II	III	IV
Ec	0.001	0.003	0.005	0.007

Fig. 24. Variation of* θ *with Ec at* $x=\frac{2}{3}$ *level

	I	II	III	IV
Ec	0.001	0.003	0.005	0.007

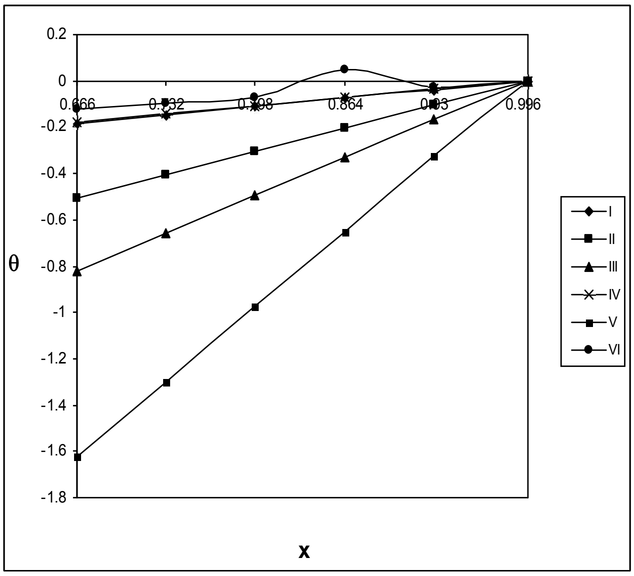

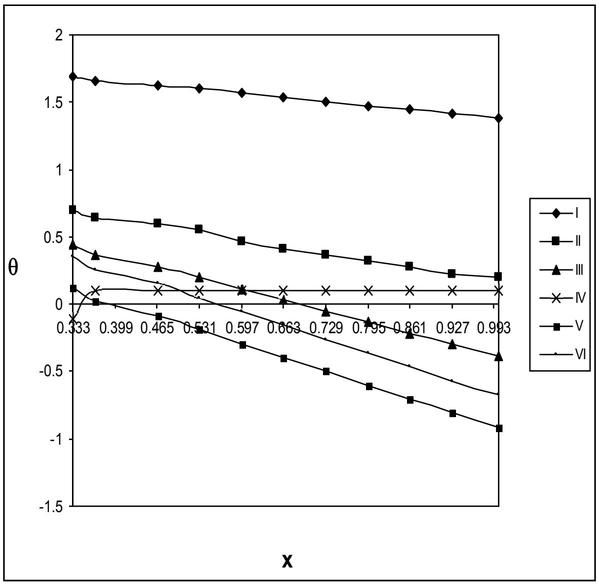

Fig. 25. Variation of* θ *with k at* $y=\frac{2h}{3}$ *level

	I	II	III	IV	V	VI
k	0.5	1.5	2.5	-0.5	-1.5	-2.5

Fig. 26. Variation of* θ *with k at* $y=\frac{h}{3}$ *level

	I	II	III	IV	V	VI
k	0.5	1.5	2.5	-0.5	-1.5	-2.5

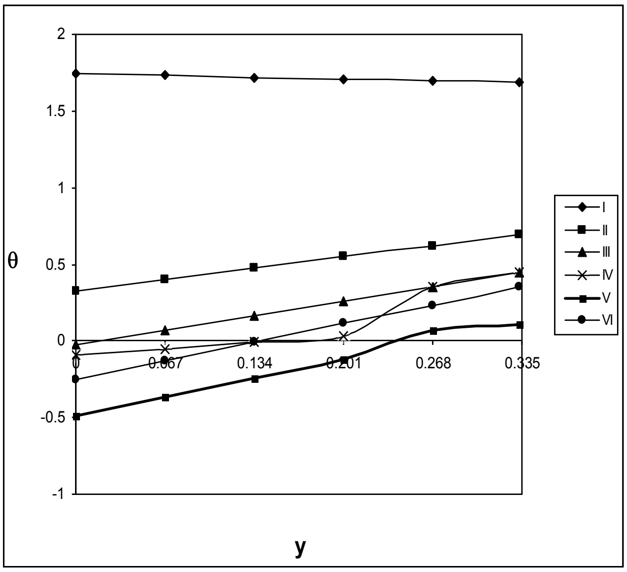

Fig. 27. Variation of θ with k at $x=\dfrac{1}{3}$ level

	I	II	III	IV	V	VI
k	0.5	1.5	2.5	-0.5	-1.5	-2.5

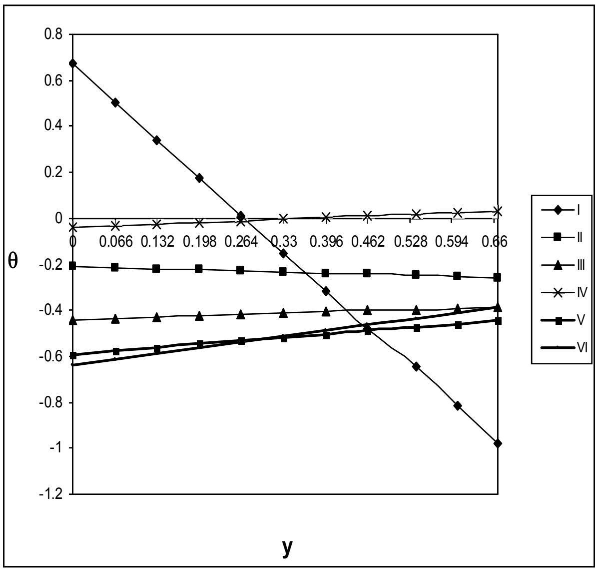

Fig. 28. Variation of θ with k at $x=\dfrac{2}{3}$ level

	I	II	III	IV	V	VI
k	0.5	1.5	2.5	-0.5	-1.5	-2.5

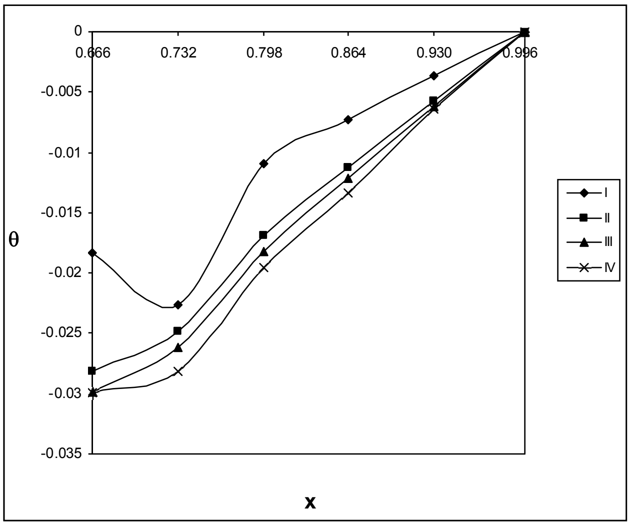

Fig. 29. Variation of θ with M at $y=\dfrac{2h}{3}$ level

	I	II	III	IV
M	5	10	15	20

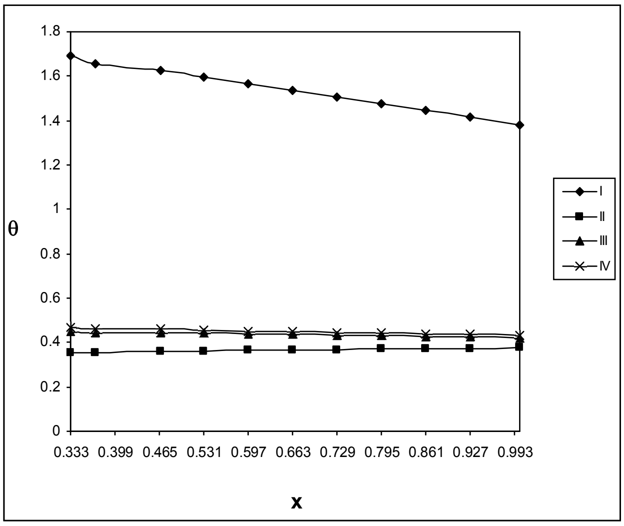

Fig. 30. Variation of θ with M at $y=\dfrac{h}{3}$ level

	I	II	III	IV
M	5	10	15	20

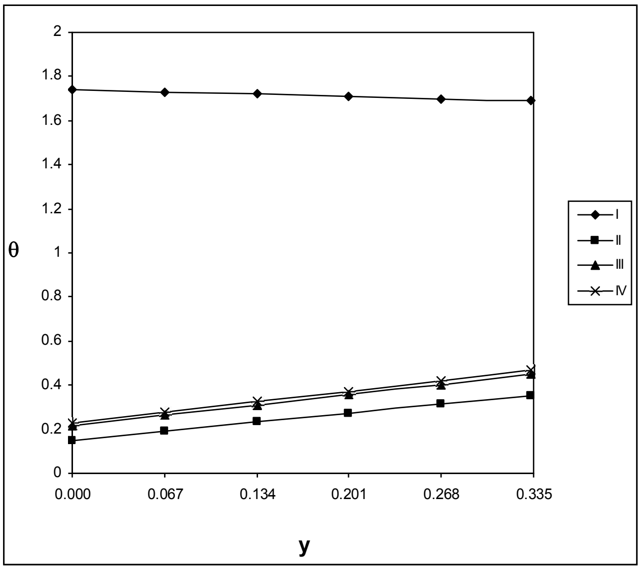

Fig. 31. Variation of θ with M at $x = \frac{1}{3}$ level

	I	II	III	IV
M	5	10	15	20

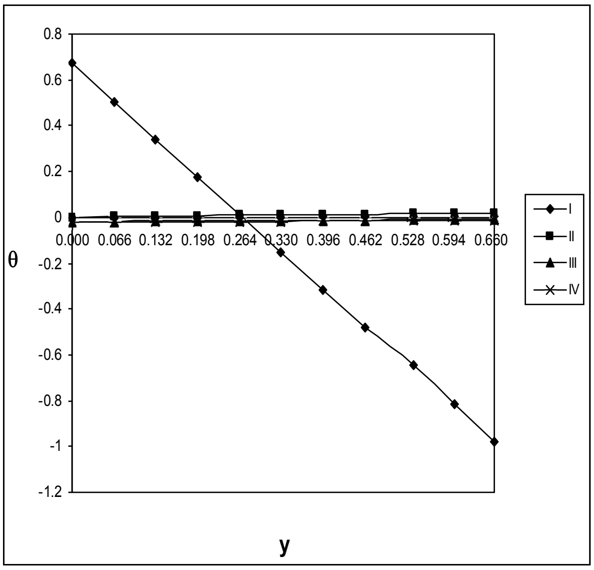

Fig. 32. Variation of θ with M at $x = \frac{2}{3}$ level

	I	II	III	IV
M	5	10	15	20

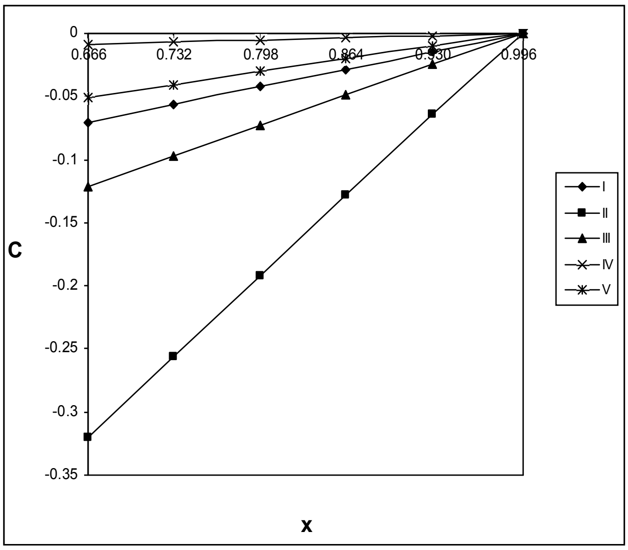

Fig. 33. Variation of C with R at $y = \frac{2h}{3}$ level

	I	II	III	IV	V
R	100	200	300	-100	-200

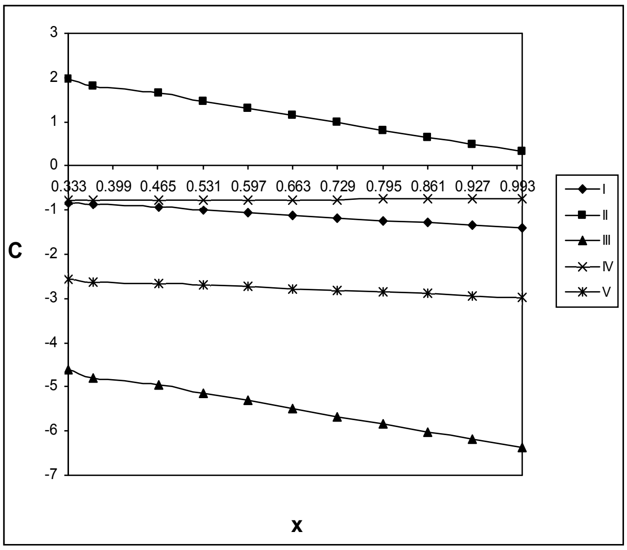

Fig. 34. Variation of θ with C at $y = \frac{h}{3}$ level

	I	II	III	IV	V
R	100	200	300	-100	-200

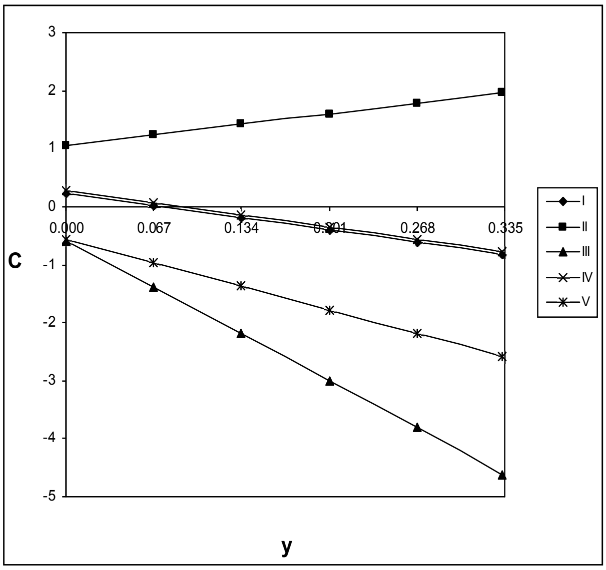

Fig. 35. Variation of C with R at $x = \frac{1}{3}$ *level*

	I	II	III	IV	V
R	100	200	300	-100	-200

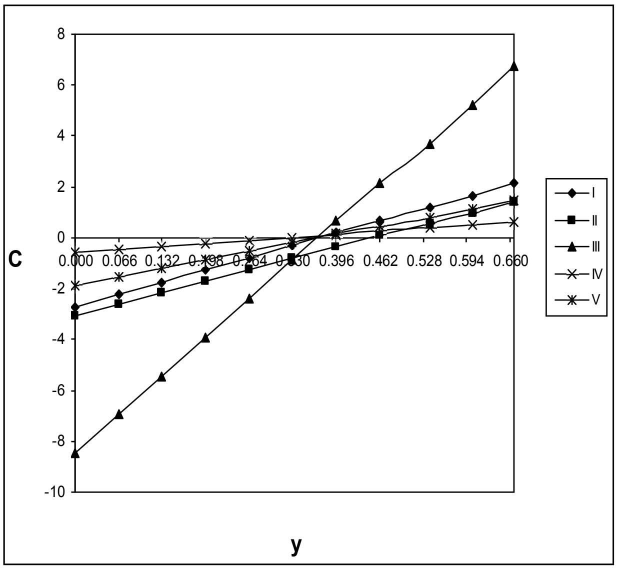

Fig. 36. Variation of C with C at $x = \frac{2}{3}$ *level*

	I	II	III	IV	V
R	100	200	300	-100	-200

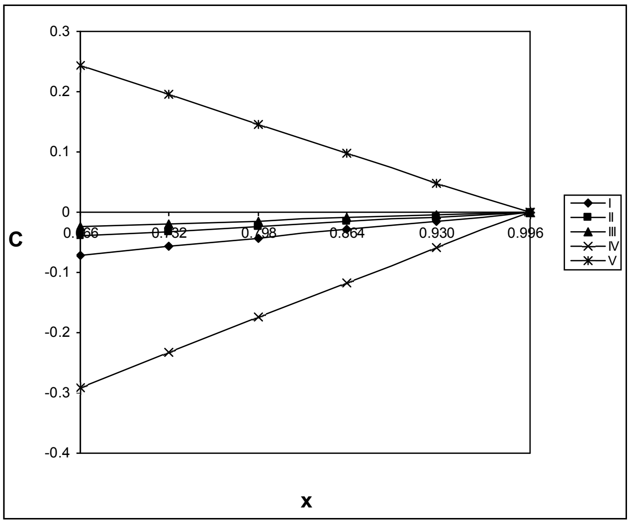

Fig. 37. Variation of C with α *at* $y = \frac{2h}{3}$ *level*

	I	II	III	IV	V
α	2	4	6	-2	-4

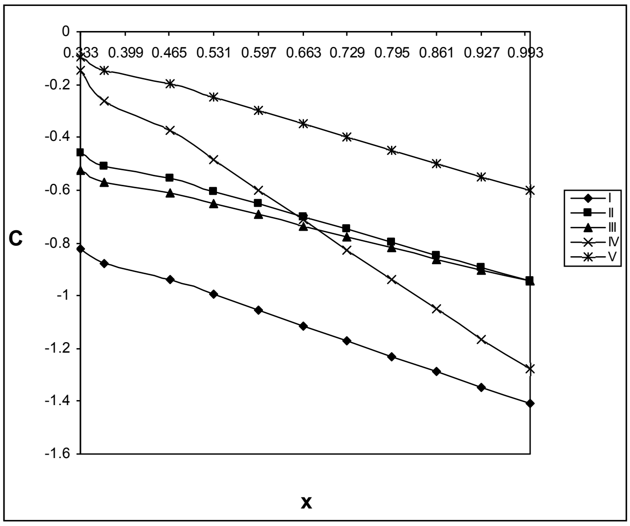

Fig. 38. Variation of C with α *at* $y = \frac{h}{3}$ *level*

	I	II	III	IV	V
α	2	4	6	-2	-4

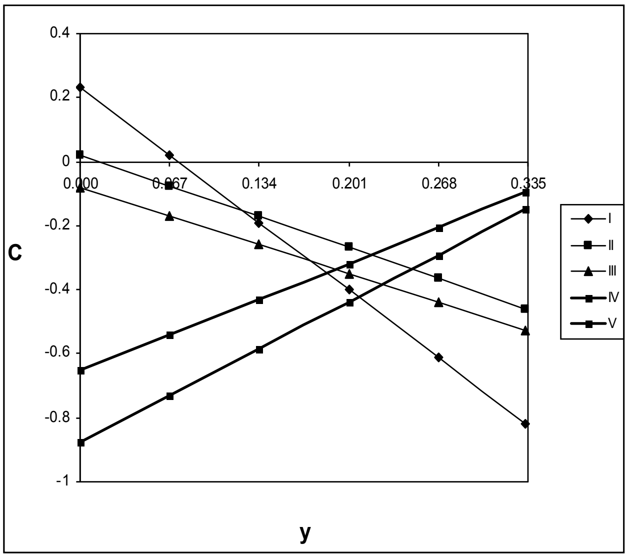

Fig. 39. Variation of C with α at $x=\dfrac{1}{3}$ level

	I	II	III	IV	V
α	2	4	6	-2	-4

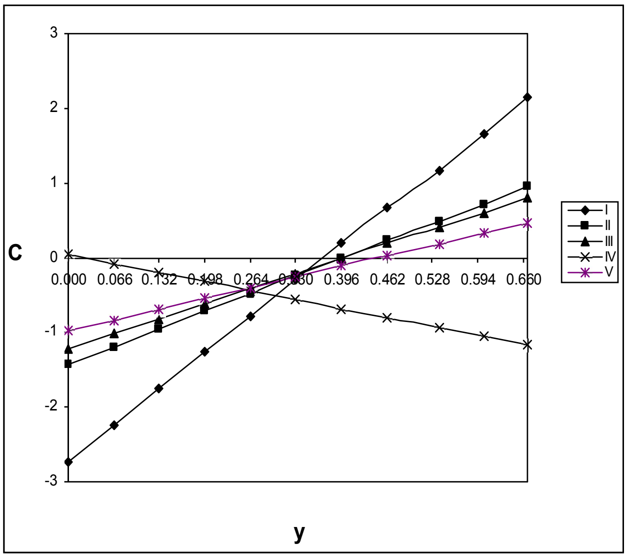

Fig. 40. Variation of C with α at $x=\dfrac{2}{3}$ level

	I	II	III	IV	V
α	2	4	6	-2	-4

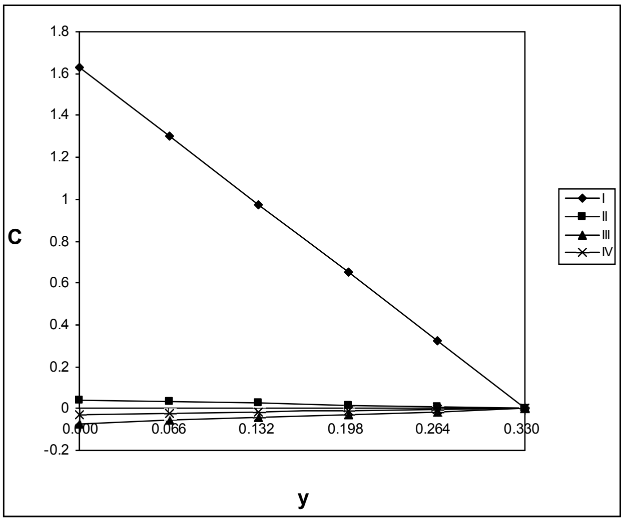

Fig. 41. Variation of C with Sc at $y=\dfrac{2h}{3}$ level

	I	II	III	IV
Sc	0.24	0.6	1.3	2.01

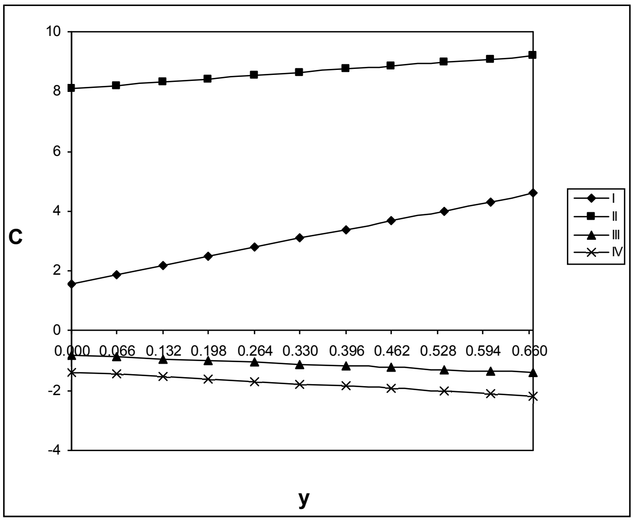

Fig. 42. Variation of C with Sc at $y=\dfrac{h}{3}$ level

	I	II	III	IV
Sc	0.24	0.6	1.3	2.01

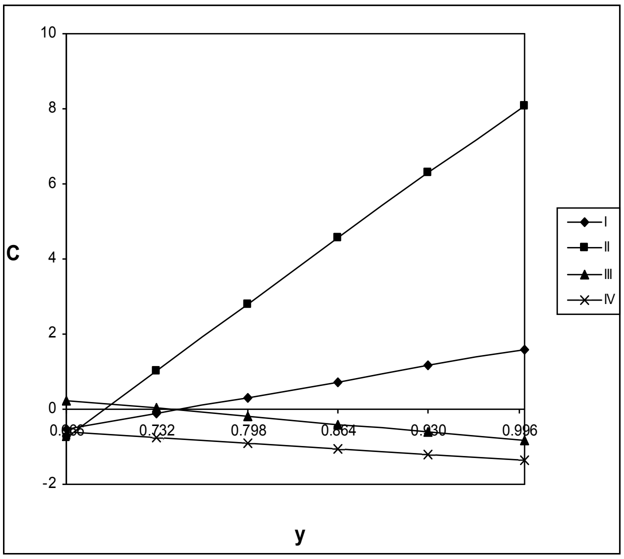

Fig.43. Variation of C with Sc at $x = \frac{1}{3}$ *level*

	I	II	III	IV
Sc	0.24	0.6	1.3	2.01

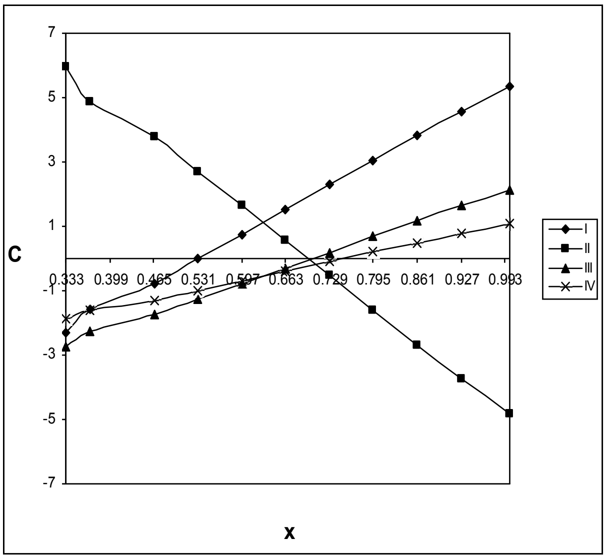

Fig. 44. Variation of C with Sc at $x = \frac{2}{3}$ *level*

	I	II	III	IV
Sc	0.24	0.6	1.3	2.01

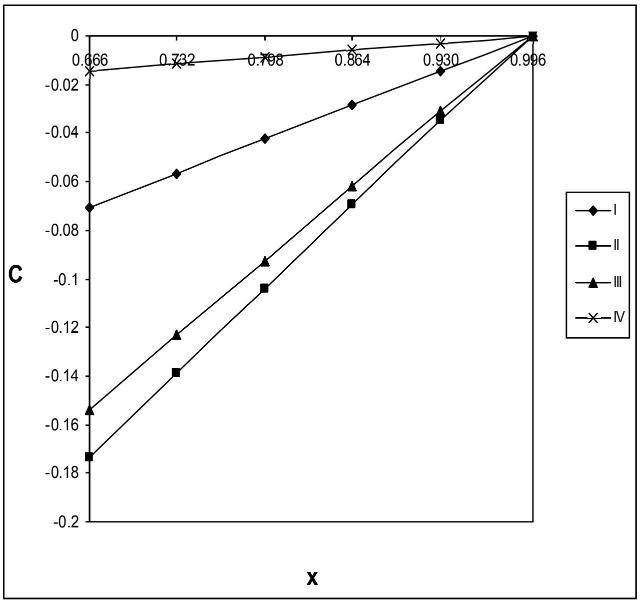

Fig. 45. Variation of C with N at $y = \frac{2h}{3}$ *level*

	I	II	III	IV
N	1	2	-0.5	-0.8

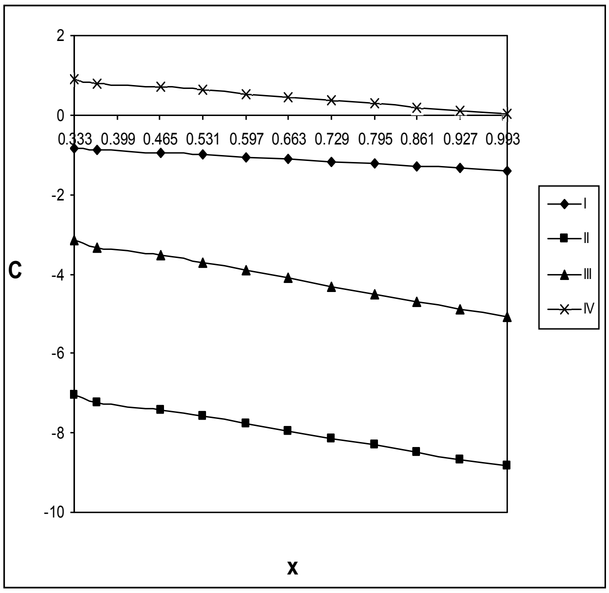

Fig. 46. Variation of C with N at $y = \frac{h}{3}$ *level*

	I	II	III	IV
N	1	2	-0.5	-0.8

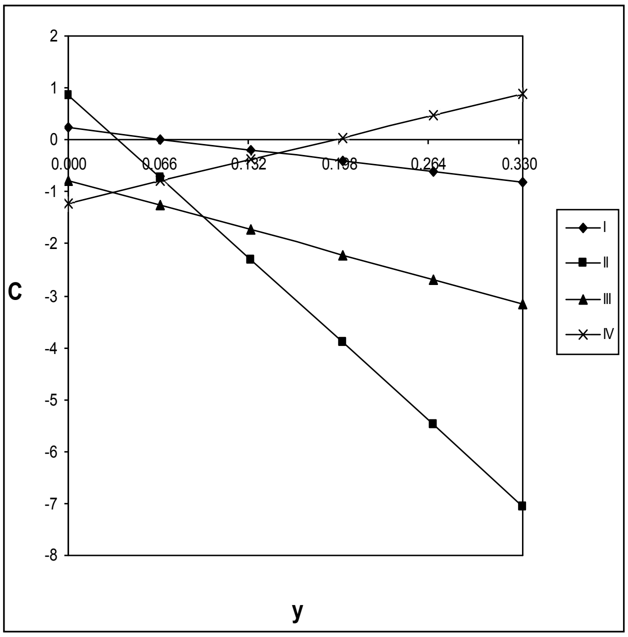

Fig. 47. Variation of C with N at $x = \frac{1}{3}$ *level*

	I	II	III	IV
N	1	2	-0.5	-0.8

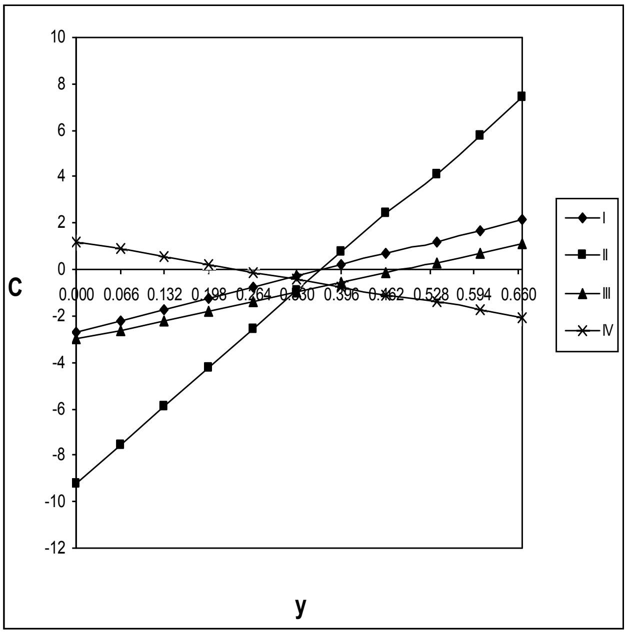

Fig. 48. Variation of C with N at $x = \frac{2}{3}$ *level*

	I	II	III	IV
N	1	2	-0.5	-0.8

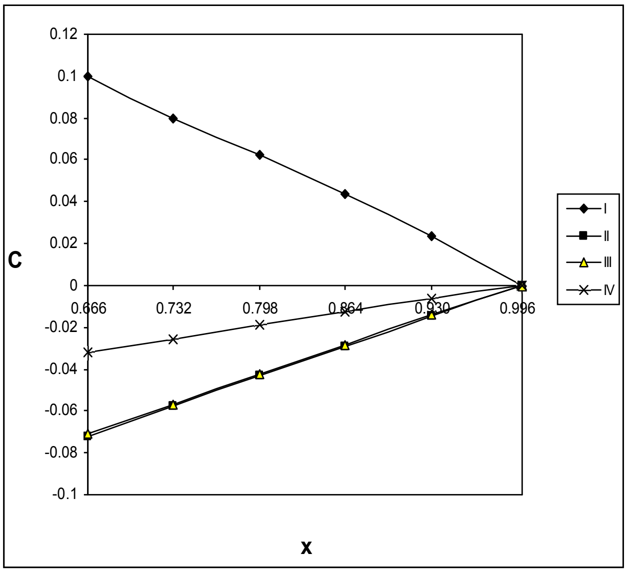

Fig. 49. Variation of C with N_1 *at* $y = \frac{2h}{3}$ *level*

	I	II	III	IV
N_1	0.01	0.03	0.05	0.07

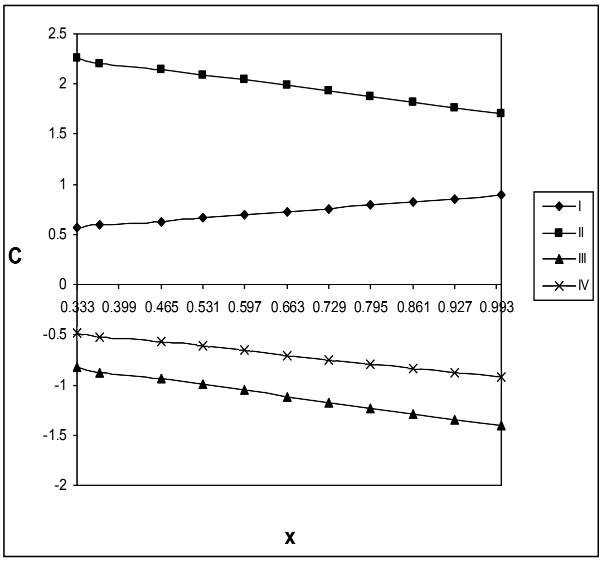

Fig. 50. Variation of C with N_1 *at* $y = \frac{h}{3}$ *level*

	I	II	III	IV
N_1	0.01	0.03	0.05	0.07

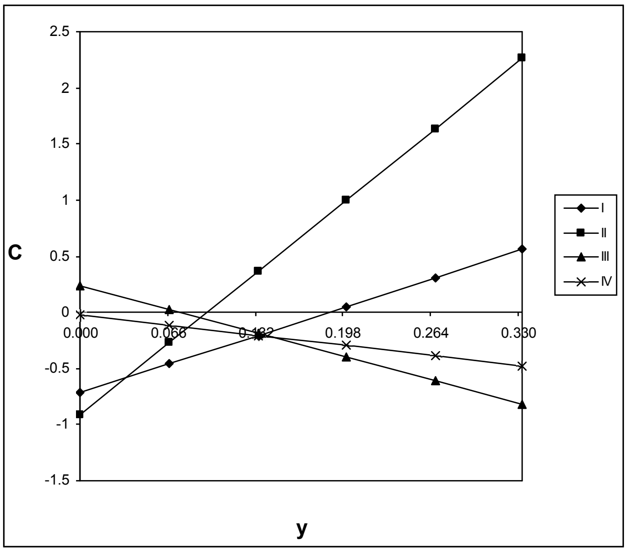

Fig.51. Variation of C with N_1 at $x = \frac{1}{3}$ *level*

	I	II	III	IV
N_1	0.01	0.03	0.05	0.07

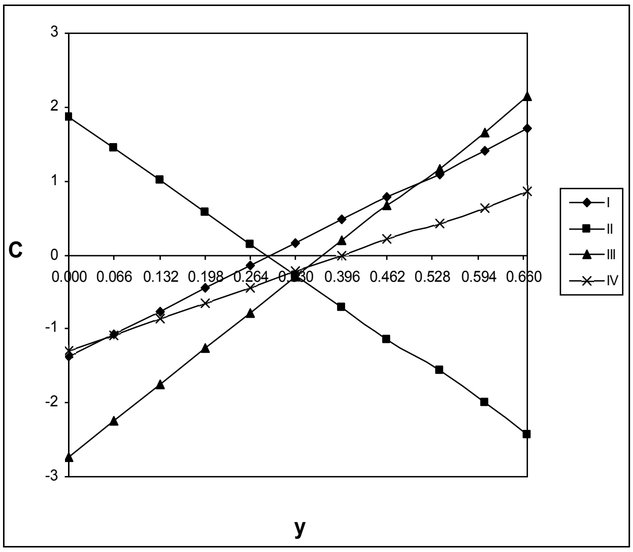

Fig. 52. Variation of C with N_1 at $x = \frac{2}{3}$ *level*

	I	II	III	IV
N_1	0.01	0.03	0.05	0.07

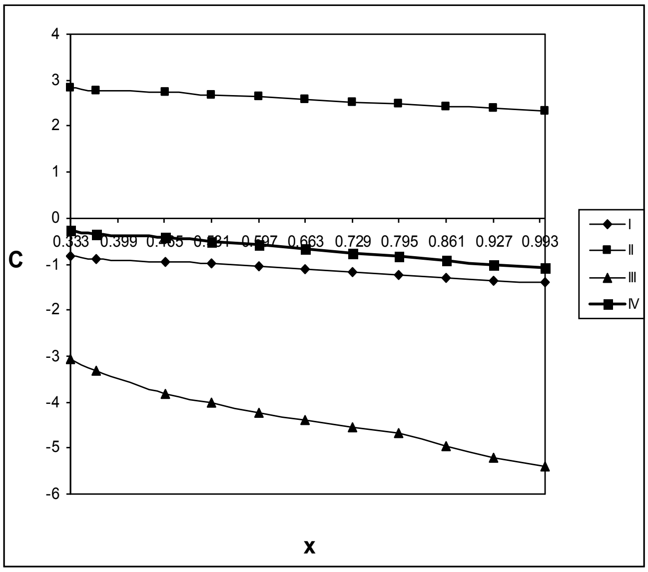

Fig. 53. Variation of C with Ec at $y = \frac{2h}{3}$ *level*

	I	II	III	IV
Ec	0.001	0.003	0.005	0.007

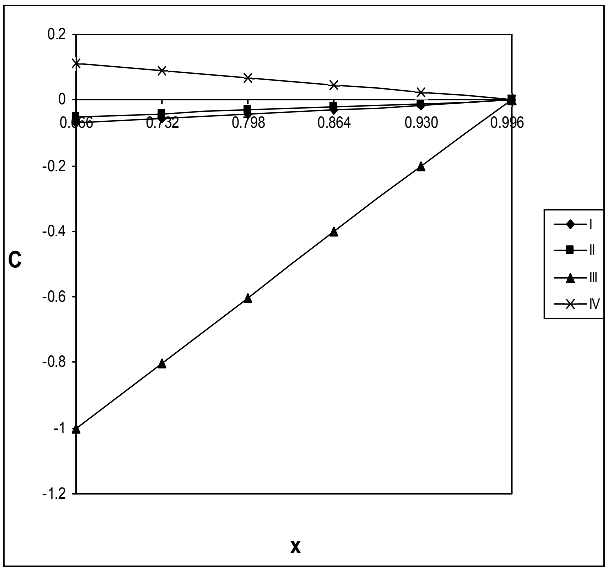

Fig. 54. Variation of C with Ec at $y = \frac{h}{3}$ *level*

	I	II	III	IV
Ec	0.001	0.003	0.005	0.007

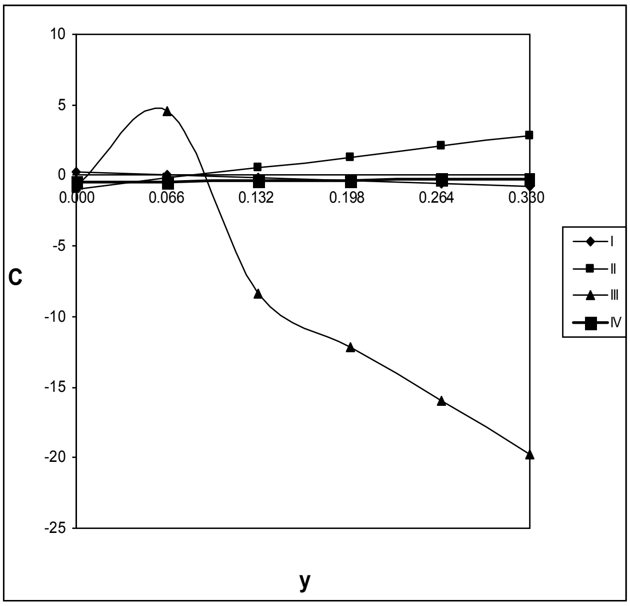

Fig. 55. Variation of C with Ec at $x = \frac{1}{3}$ *level*

	I	II	III	IV
Ec	0.001	0.003	0.005	0.007

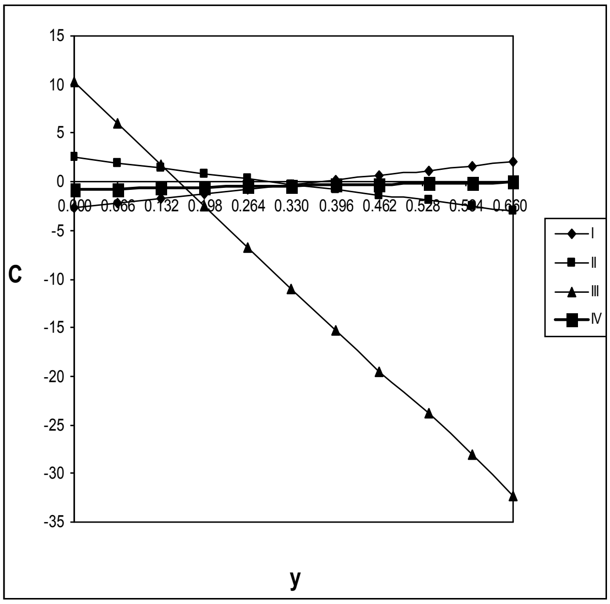

Fig. 56. Variation of C with Ec at $x = \frac{2}{3}$ *level*

	I	II	III	IV
Ec	0.001	0.003	0.005	0.007

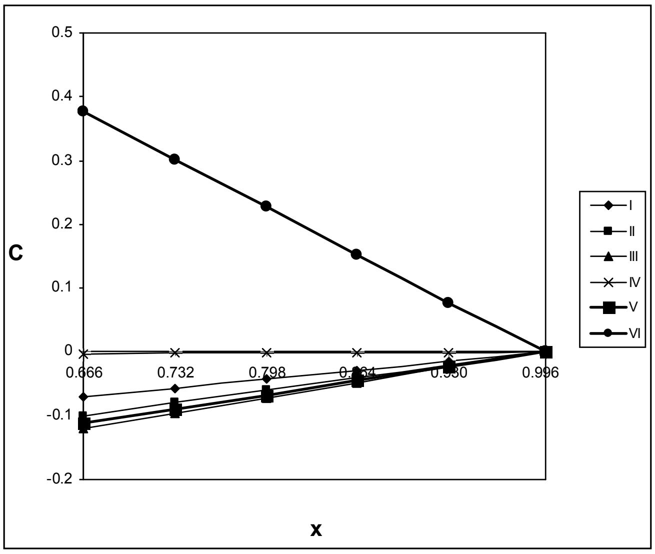

Fig. 57. Variation of C with k at $y = \frac{2h}{3}$ *level*

	I	II	III	IV	V	VI
k	0.5	1.5	2.5	-0.5	-1.5	-2.5

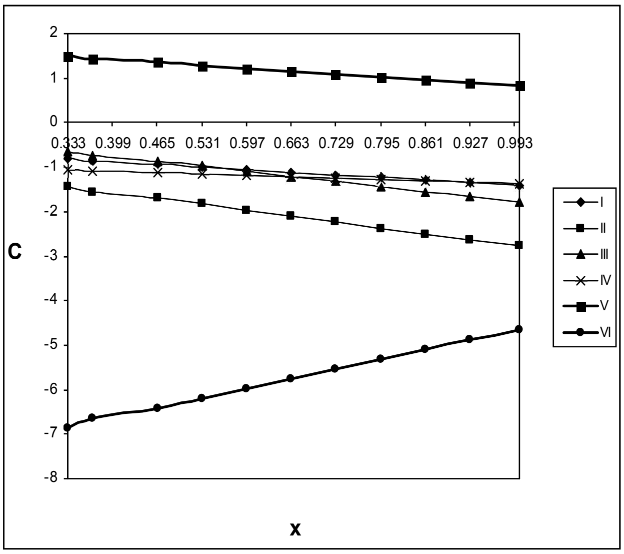

Fig. 58. Variation of C with k at $y = \frac{h}{3}$ *level*

	I	II	III	IV	V	VI
k	0.5	1.5	2.5	-0.5	-1.5	-2.5

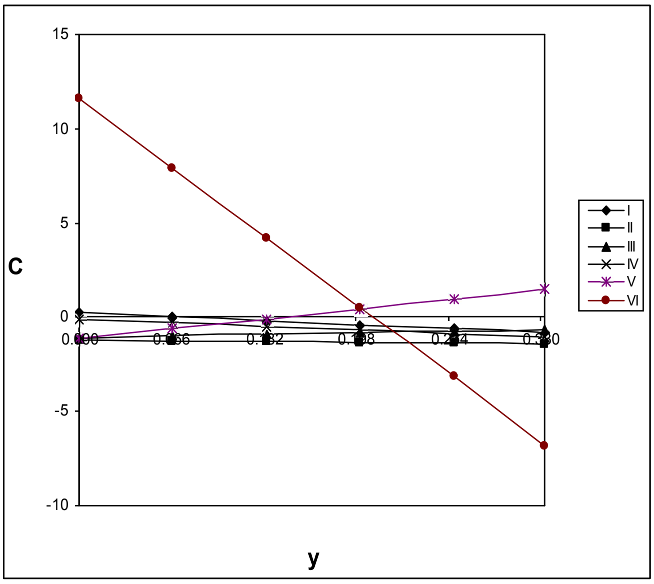

Fig. 59. Variation of C with k at $x = \frac{1}{3}$ *level*

	I	II	III	IV	V	VI
k	0.5	1.5	2.5	-0.5	-1.5	-2.5

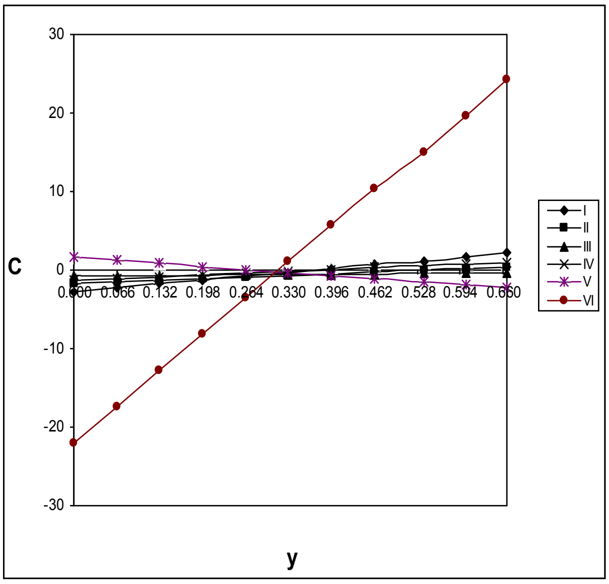

Fig. 60. Variation of C with k at $x = \frac{2}{3}$ *level*

	I	II	III	IV	V	VI
k	0.5	1.5	2.5	-0.5	-1.5	-2.5

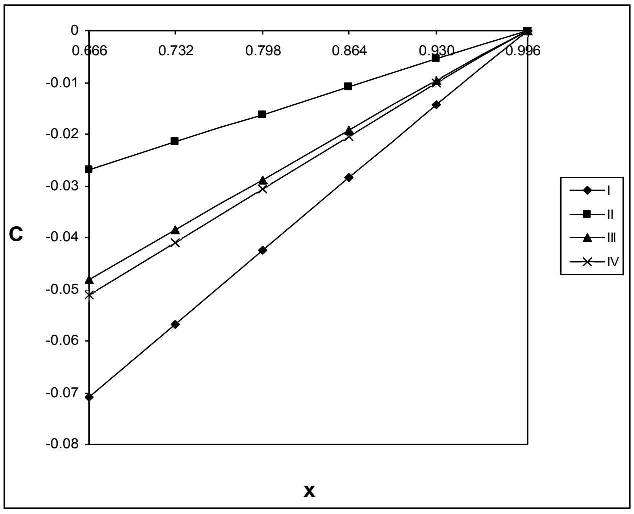

Fig. 61. Variation of C with M at $y = \frac{2h}{3}$ *level*

	I	II	III	IV
M	5	10	15	20

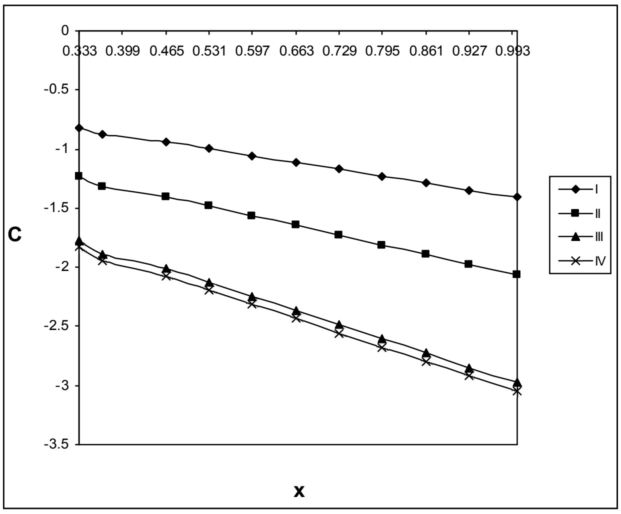

Fig. 62. Variation of C with M at $y = \frac{h}{3}$ *level*

	I	II	III	IV
M	5	10	15	20

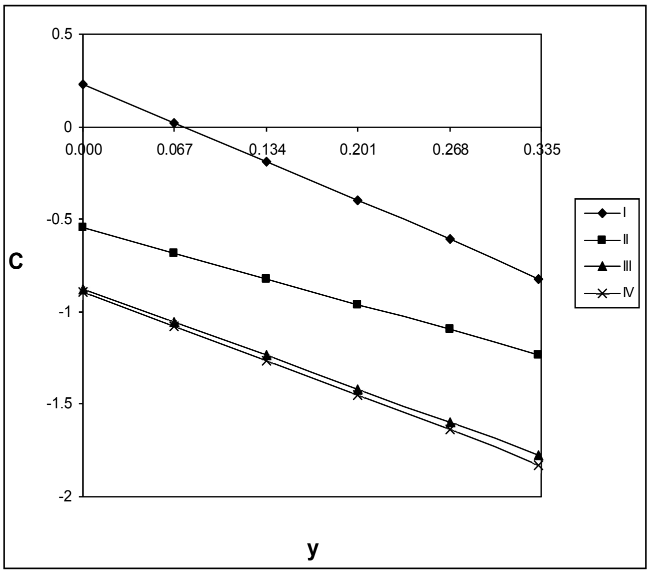

Fig. 63. Variation of C with M at $x=\frac{1}{3}$ *level*

	I	II	III	IV
M	5	10	15	20

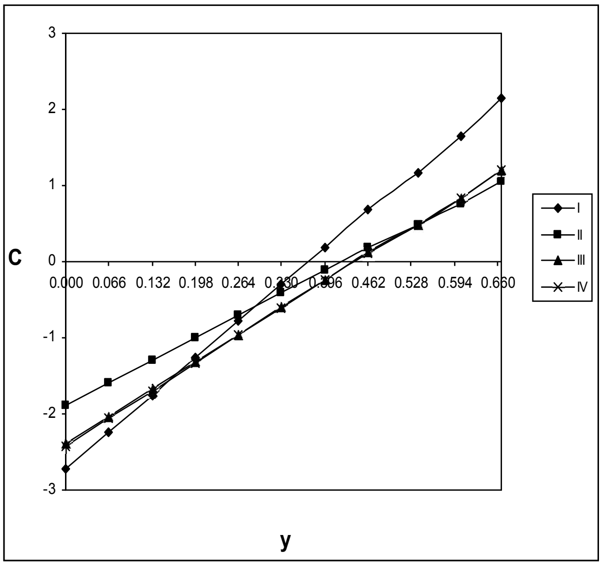

Fig. 64. Variation of C with M at $x=\frac{2}{3}$ *level*

	I	II	III	IV
M	5	10	15	20

REFERENCES

[1] Bankvall, C.G, "Natural convective heat transfer in a insulated structures," *Lundinst. Tech. Report 38*, pp. 1-149, 1972.
[2] Bankvall, C.G, "Heat transfer in fibrous material," *J. Test. E*, vol. 3, pp. 235-243, 1973.
[3] C. E. Hickox and D. K. Gartling, "A numerical study of natural convection in a horizontal porous layer subjected to an end-to-end temperature difference," *ASME J. Heat Transfer*, 103, 797–802, 1981.
[4] Hiroxhi Iwai, Kazuyoshi nakabe, Kenjiro Suzuki, "Flow and Heat transfer characteristics of backward-facing step laminar flow in a rectangular duct," *Int. J. Heat and Mass transfer*, vol. 43, pp. 457-471, 2000.
[5] J. Kakutani, *J. Phys. Soc, Japan*, vol. 13, p. 1504, 1958.
[6] Prasad, V. and Kulacki, F.A, "Natural convection in a vertical porous annulus," *Int. J. Heat mass transfer*, vol. 27, pp. 207-219, 1984.
[7] K. Padmalatha, Ph.D. Thesis on "Finite element analysis of laminar convection flow through a porous medium in ducts," *S.K. University, Anantapur, (A. P) India*, 1997.
[8] Padmavathi, A., "Finite element analysis of the Convective heat transfer flow of a viscous in compressible fluid in a Rectangular duct with radiation, viscous dissipation with constant heat source," *Jour. Phys and Appl.Phys*., vol. 2, 2009.
[9] Prasad, V. and Kulacki, F.A. , "Convective heat transfer in a rectangular porous cavity effect of aspect ratio flow structure and heat transfer," *ASME Journal of heat transfer*, vol. 106, pp. 158-165, 1984.
[10] Poulikakos, D. and Bejan, A., "Natural convection in vertically and horizontally layered porous media heated from side," *Int. J. heat and mass transfer*, vol. 26, pp. 1805-1813, 1983.
[11] Rangareddy, M., "Heat and Mass transfer by Natural convection through a porous medium in ducts," *Ph.D thesis, S.K. University, Anantapur*, 1997.
[12] Seki. N., Fukusako. S and Inaba, H., "Heat transfer in a confined rectangular cavity packed with porous media," *Int. J. of heat and mass transfer*, vol. 21, pp. 985-989, 1981.
[13] Sivaiah, S., "Thermo-Diffusion effects on convective heat and mass transfer through a porous medium in Ducts," *Ph.D thesis, S.K University, Anantapur, India*, 2004.
[14] Bejan, A., "On the boundary layer region in a vertical enclosure filled with a porous medium," *letters heat and mass transfer*, vol. 6, pp. 93-102, 1979.
[15] Beckermann C, Ramadhyani, S, and Viskanta, R., "Natural convection flow and heat transfer between fluid layer and a porous layer inside a rectangular enclosure," *Journal of heat transfer*, vol. 109, p, 363, 1987.
[16] Cheng K.S. and J.R. Hi., "Steady, Two-dimensional, natural convection in rectangular enclosures with differently heated walls," *Transaction of the ASME*, vol. 109, p, 400, 1987.
[17] Chan, B.K.C, Ivey, U.M and Barry, J.M., "Natural convection in enclosed porous medium with rectangular boundaries," *ASME journal of heat transfer*, vol. 92, pp. 21-27, 1970.
[18] Holst, P.H., "Transient three dimensional natural convection in confined porous media," *Int. J. Heat Mass transfer*, vol. 15, pp. 72-89, 1972.
[19] Joseph, J. Savino and Robert Siegel., "Laminar forced convection in Rectangular channels with unequal Heat addition on adjacent sides," *Int. J. Heat Mass transfer*, vol. 71, pp. 733-741, 1964.
[20] Kermant, B.C.C., "Natural convection flow and heat transfer between a fluid layer and a porous layer inside a rectangular enclosure," *Heat Transfer Laboratory, Purdue, University*, Indiana.
[21] Kamotani, Wang. L.W. Ostrach. S. and Jiang, H.D., "Experimental study of natural convection in shallow enclosures with horizontal temperature and concentration gradients," *Int. J. Heat Mass transfer*, vol. 28 pp. 165-173, 1985.
[22] Lauriant, F., "Natural convection and radiation on enclosure partially, filled with a porous insulation," *ASME*, pp. 84-107, 1984.
[23] Morrison, F. A., "Transient multiphase Multi component flow in porous media," *Int. J. Heat mass transfer*, vol. 16, pp. 2331-2341, 1973.
[24] Verschoor, J.D, and Greebler, P., "Heat Transfer by gas conduction and radiation in fibrous insulation," *Trans. Am. Soc. Mech. Engrs,* pp. 961-968, 1952.
[25] Ribando, R.J. and Torrance, K.E., "Natural convection in a porous medium effects of confinement, variable permeability and thermal boundary conditions," *Trans. Am. Soc. Mech. Engrs. Series. C.J. Heat Transfer,* vol. 98, pp. 42-48, 1976.
[26] Rubin, A. and Schweitzer, S., "Heat transfer in porous media with phase change," *Int. J. Heat Mass Transfer*, vol. 15, pp. 43-59, 1972.
[27] Bankvall, C.G., "Natural convective in vertical permeable space," *Warme-and staffubertragung*, vol. 7, pp. 22-30, 1974.
[28] Burns, P.J, Chow, L.C. and Chen, S., *Int. J. Heat and Mass transfer,* vol. 20, pp. 919-926, 1926.
[29] Teoman Ayhan, Hayati Olgum, and Betul Ayhan, "Heat transfer and flow structure in a Rectangualr channel withwing -1. type vortex Generator," *Tr. J. of Engineering and Environmental Science*, pp. 185-195, 22, 1998.

[30] Ham-Chien Chiu, Jer-Huan Jang, Wei-Monyan, "Mixed convection heat transfer in Horizontal rectangular ducts with radiation effects," *Int. Journal of Heat Mass transfer 50*, pp. 2874-2882, 2007.

[31] Chittibabu. D., Prasada Rao. D.R.V., Krishna D.V., "Convection flow through a porous medium in ducts," *Act science Indica,* vol. 30 2M, pp. 635-642, 2006.

[32] Ostrach. S., Jiang. H.D., Kamotani. Y., "Thermo solutal convection in shallow enclosures," in *ASME, JSME thermal Engineering Joint Confernece,* Hawali, 1987.

[33] R. Viskanta, T.L. Bergman, F.P. Incropera, "Double diffusive natural convection," in: *S. Kakac, W. Aung, R. Viskanta (Eds.), Natural Convection: Fundamentals and Applications, Hemisphere, Washington, DC*, pp. 1075–1099, 1985.

[34] Lee. L., Hyun. M.T., Kim. K.W., "Natural convection in confined fluids with combined horizontal temperature and concentration gradients," *Int. J. Heat Mass Transfer 31*, pp. 1969-1977, 1985.

[35] Hyun. J.M., Lee. J.W., "Double – diffusive convection in a rectangle with cooperating horizontal gradients of temperature and concentration gradients," *Int. J. Heat Mass transfer 33*, pp. 1605-1617, 1990.

[36] Trevisan, O.V. Bejan A., "Mass and heat transfer by natural convection in a vertical slot filled with porous medium," *Int. J. Heat Mass Transfer,* vol.29 403-415, 1986.

[37] Shanthi, G., "Numerical study of double diffusive flow of a viscous fluid through a porous medium in channels/ducts wit heat sources," *Ph. Thesis , S. K. Universtity,* Anantapur, 2010.

[38] Brinkmann, H.C., "A calculation of the viscous force external by a flowing fluid on a dense swarm of particles," *Applied science Research, Ala*, p 81, 1948.

[39] Verschoor, J.D, and Greebler, P., "Heat Transfer by gas conduction and radiation in fibrous insulation," *Trans. Am. Soc. Mech. Engrs,* pp. 961-968, 1952.

[40] Badruddin, I. A, Zainal, Z.A, Aswatha Narayana, Seetharamu, K.N., "Heat transfer in porous cavity under the influence of radiation and viscous dissipation," *Int. Comm. In Heat & Mass Transfer 33*, pp. 491-499, 2006.

[41] Nagaradhika V., "Mixed convective heat transfer through a porous medium in a Corrugated channel/ducts," *Ph.D. thesis, S.K. University,* 2010.

[42] Reddaiah, P., "Heat and Mass Transfer flow of a viscous fluid in a duct of rectangular cross section by using finite element analysis," *European J. Of Prime and Applied Mathematics*, 2010.

[43] Lee L.W., Hyun. J. M., "Double – diffusive convection in a rectangle with opposing horizontal and concentration 8 gradients," *Int. J. Heat, Mass transfer*, vol. 33, 1990.

[44] Saffman, P.G., *Studies in Applied Mathematics*, vol. 50, p. 537, 1969.

[45] San. J., "Natural convection in a rectangular porous cavity with constant heat flux as vertical wall," *Trans. Of ASME*, vol. 106, p. 252, 1984.

[46] Trevisan. O.V., Bejan. A., "combined heat and mass tr ansfer by natural convection in a vertical enclosure," *ASME, J. Heat Transfer, 19*, pp.104-112, 1987.

[47] Turner. B.C, and Flack R.D., "The experimental measurement of natural convective heat transfer in rectangular enclosures with concentrated energy source," *Trans. Of ASME,* vol. 102, pp. 236-242, 1980.

[48] Tien C.L. and Hong. J. T., "Natural convection in porous media under non-darcion and non-uniform permeability convections," in *Natural Convection S. Kakac, et. al., (eds), Wemisphere, Washington, D.C.,* 1985.